Journal of Vibration Engineering & Technologies (2021) 9:2047–2071
https://doi.org/10.1007/s42417-021-00348-0

ORIGINAL PAPER

An Analytical Investigation on Linear and Nonlinear Vibrational Behavior of Stiffened Functionally Graded Shell Panels Under Thermal Environment

Anubhav Kumar[1] · Dinesh Kumar[1] · Kanishk Sharma[2]

Received: 8 May 2021 / Revised: 24 June 2021 / Accepted: 26 June 2021 / Published online: 28 July 2021

Abstract

Purpose In this paper, an analytical investigation of the nonlinear dynamic response and vibrational behavior of stiffened and unstiffened FGM shell panels of different geometries under thermo-mechanical loading is presented.

Methods The kinematic relations considered for shell panels are in accordance with the first-order shear deformation theory along with von Kármán geometrical nonlinearities, and the contribution of stiffeners is considered based on smeared stiffener technique. The nonlinear governing equations of motion for eccentrically stiffened FGM shell panels are derived using Hamilton's principle. Navier's functions are assumed to satisfy the prescribed boundary conditions, whereas Galerkin and fourth-order Runge–Kutta methods are employed to attain nonlinear dynamic responses.

Results After establishing the accuracy of the present analytical formulation by comparing the results with the existing literature, various numerical studies are conducted to divulge the impact of parameters such as shell geometries, stiffeners, material inhomogeneity, and temperature difference on the nonlinear dynamic response and vibrational behavior of simply-supported FGM shell panels.

Conclusions It is revealed that among the un-stiffened as well as stiffened FGM shell panels, the spherical shell panel exhibits the highest natural frequency with the lowest vibration amplitude, whereas the lowest natural frequency with the highest amplitude is depicted by the hyperbolic-paraboloidal shell panel. Moreover, the effects of the increase in the temperature difference across the thickness and the power law index are to reduce the natural frequency and to increase the amplitude of dynamic response, irrespective of the geometry of shell panels. Further, the effect of damping on the dynamic behavior of the FGM shell panel is initially indistinguishable; however, after a few time periods the damping is found to have a considerable effect on its dynamic response.

Keywords Functionally graded material (FGM) · Nonlinear dynamic response · Stiffened shallow shell panels · Galerkin method · Thermo-mechanical

Introduction

Out of the many basic structural elements like beam, plate, and shell, thin-walled curved shells are being used in many engineering applications in mechanical, civil, marine, and aeronautical fields because of their many advantages such as high strength-to-weight ratio, high stiffness, high efficiency of load-carrying behavior, structural integrity, high reserved strength, and aesthetic look [1]. Moreover, to further enhance their performance, these thin-walled shells have been reinforced with stiffeners/ribs. The assimilation of the stiffeners provides a promising advantage of controlling the vibration response by altering the natural frequencies of these shell structures with the enhanced stiffness, without increasing

✉ Dinesh Kumar
dkumar.mech@mnit.ac.in

Anubhav Kumar
2014rme9061@mnit.ac.in

Kanishk Sharma
kanishksharma2009@gmail.com

1 Mechanical Engineering Department, Malaviya National Institute of Technology, Jaipur 302 017, India

2 Mechanical Engineering Department, JECRC University, Jaipur 303905, India

the shell thickness. Nevertheless, the dynamic behavior of these structures is quite complex due to which there is an overwhelming research interest pertaining to the linear and nonlinear vibration analysis of stiffened shell structures. In the early exploratory attempts, Miller [2] used the energy method to calculate natural frequencies and mode shapes of a circular cylindrical shell uniformly stiffened with closely spaced stiffeners and frames, and Hoppmann [3] described the experimental method and verified the existing theoretical results experimentally for orthogonally stiffened cylindrical shells. The free vibration of ring stiffened conical shell based on linear shell theory was presented by Weingarten [4].

The effects of eccentrically placed stiffeners over the dynamic response of plate and shell structures were investigated by McElman et al. [5]. In all these studies [2–5], and reviewed in [6], on free vibration response of isotropic shells, equidistant closely spaced stiffeners were simplified by uniformly averaging the effect of stiffeners over the entire shell surface. Thereafter, the effects of shell geometry, the position of multi-directional stiffeners, and the boundary conditions on the free vibration behavior of stiffened isotropic shells were also revealed in many subsequent studies [6]. Later on, Nayak and Bandyopadhyay [7]analyzed the free vibration of doubly curved shallow shells using a finite element method with the eight-/nine-node doubly curved iso-parametric thin shallow shell element and the three-node curved iso-parametric beam element. Free vibration of various types of shallow and deep stiffened shell structures was studied using a new stiffened shell element by Samanta et al. [8], and thereafter, Qu et al. [9] presented a modified variational approach to analyse vibration of ring-stiffened conical–cylindrical shells with different boundary conditions.

In addition to the aforementioned studies on isotropic shells, the increased uses of composite materials in many engineering applications generated the interest of researchers in composite structures, including composite shells. Attributable to the wide applicability, free vibration and dynamic behavior of composite shells have drawn overwhelming research interest of researchers over the last four decades[10, 11]. Very recently, Tran et al. [12] implemented FSDT for the static and free vibration analysis of stiffened cross-ply laminated composite doubly-curved shallow shells. TSDT based finite element analysis of free vibration of doubly curved laminated composite shells with cutout was presented by Chaubey et al. [13]. Guo et al. [14] performed free and forced vibration analysis of composite laminated doubly-curved shells, based on FSDT using a domain decomposition method. Ni et al. [15] proposed FSDT based semi-analytical approach to investigate free vibration of stiffened composite laminated shells of revolution with classical and elastic boundaries. In the study, of the nonlinear vibration of fiber-reinforced polymer composite cylindrical shells Li et al. [16] employed Love's shell theory including geometric nonlinearities and thermal effect.

Despite the many preferable properties of laminated composites, the abrupt change in material composition at the interface provoke high interfacial stresses leading delamination, matrix cracking, and adhesive bond separation failure, under critical loading conditions at elevated temperature. While looking to overcome the limitations of traditional composite materials, a new class of composites, namely Functionally Graded Materials (FGMs) were developed by the Japanese material Scientists in 1984 [17]. FGMs are inhomogeneous composite materials with the composition of constituting materials varying smoothly and continuously in one or more spatial directions according to some mathematical function, and hence, eliminating any problem at interface caused by properties mismatch. Usually, FGMs have ceramic and metal constituents, and the preferable material properties at a particular location is tailored and achieved by controlling the volume fractions of these constituent materials. It is found in many investigations that functionally graded structures show much better structural performance as compared to homogenous materials under thermo-mechanical loading conditions [17–19]. Further, the FGMs shells are most suitable for important engineering structures such as thermal protection systems in space vehicles, thrust chamber of aero-structures, rocket engine components, turbine blades, etc. [20–22]. As reported by Punera and Kant [23] in their recently published review article that in the last 2–3 decades, many investigations have been carried out to study vibration and dynamics responses of FGM shells (i.e., plate, circular/elliptical cylindrical, spherical, hyperbolic-paraboloidal) without and with stiffeners using different shell theories (i.e., Love shell theory/CST, shear deformation theories, normal/higher-order theories) with different analytical and numerical techniques.

It is noteworthy that in the classical shell theories, rotary inertia and transverse shear effects are disregarded as a consequence of which these theories overestimate the natural frequencies for moderately thick shells, therefore the results from CST can't be relied on much, especially for thick shells. Thereby to consider the transverse shear effects and to predict the free vibration response of moderately thick FGM shell structures, many researchers adopted FSDT (first-order shear deformation theory). Kim [24] analyzed free vibration characteristics of oblique-edged FGM cylindrical shell using the Rayleigh–Ritz method. Khayat et al. [25] used the semi-analytical finite strip method along with different shell theories to examine the free vibration response of stiffened FGM cylindrical shells. Free vibration characteristics of FG porous spherical shell were determined by Li et al. [26] using the energy method utilizing FSDT. Kumar et al. [27] presented a mathematical model based on FSDT to investigate the free vibration of eccentrically stiffened doubly curved functionally graded shallow shells with simply supported boundary conditions and subjected to the thermo-mechanical loading.

It is well known that the linear free vibration analysis is restricted to the small displacements and just provides a first approximation of the actual behavior; however, the thin FGM structures with material complexity may exhibit large amplitude vibration response especially under the effects of external excitations. Therefore it becomes imperative to incorporate the nonlinearity in the dynamic analysis of FGM structures and being reflected in a number of studies, for instance, Alijani et al. [28] presented primary and sub-harmonic responses of FGM doubly curved thin shallow-shells using Donnell's nonlinear kinematic relationships. A perturbation-based solution methodology was presented to investigate the nonlinear thermos-mechanical vibration response of FGM shell structures by Shen et al. [29, 30]. In addition to the analytical methodology, FEM is also applied by Kar and Pandya [31, 32] to compute nonlinear free mechanical and thermal vibration responses of doubly curved shallow shells. Recently, Hashemi et al. [33]implemented the Lindstedt-Poincare technique to obtain an analytical solution for nonlinear vibrations of the functionally graded plate.

It is observed that the works pertaining to the nonlinear vibration of stiffened FGM shells are comparatively less [34–37]. Further, it is also revealed that the nonlinear dynamic analysis of stiffened FGM shells is mostly carried out by using Volmir's assumption and the rotary inertia effects are ignored. However, the present analysis is carried out by solving all five simultaneous equations, while considering the effects of both rotary inertia and transverse shear deformations. Hence, the present method can provide more accurate results as compared to the aforementioned studies. A further advantage of the present generalized method is its simplicity that can be adopted to analyze thin to moderately thick shell panels of different geometries.

Contemplating the aforementioned facts, the present work is intended to explore analytically the free and forced vibration characteristics of FGM shell panels to divulge the impact of geometrical nonlinearity, rotary inertia, shell geometries, stiffeners orientation, thermal environment, temperature-dependent material properties, and other geometrical as well as material parameters on the natural frequency, frequency-amplitude relations, and force-amplitude curves.

Analytical Formulation

Nomenclatures

$x,\ y$ and z	Cartesian co-ordinate axes.
t	Time
a, b and h	Length, width and thickness of the shell, respectively
R_x, R_y	Radius of principal curvatures in xz and yz planes, respectively
h_x, h_y	Height of stiffeners along x and y directions, respectively
b_x, b_y	Width of stiffeners along x and y directions, respectively
$n_x,\ n_y$	Number of stiffeners along x and y directions, respectively
A_x, A_y	Area of cross-sections of stiffeners along x and y directions, respectively
e_x, e_y	Eccentricity of stiffeners along x and y directions, respectively
$I_{xx},\ I_{yy}$	Area moment of inertia of stiffeners along x and y direction, respectively
T	Temperature in K
E_c, E_m, and E_0	Young's moduli of ceramic, metal and stiffeners materials, respectively
ρ_c, ρ_m, and ρ_0	Mass densities of ceramic, metal and stiffeners materials, respectively
$\alpha_c,\ \alpha_m$	Thermal expansion coefficients of ceramic and metal, respectively
κ_c, κ_m	Thermal conductivity of ceramic and metal, respectively
ν	Poisson ratio
V_c, V_m	Volume fractions of ceramic and metal, respectively
k	Power law index
u, v, and w	Displacements corresponding to x, y and z directions, respectively
ϕ_x, ϕ_y	Rotations with respect to y and x axes, respectively
m, n	Half wave number
$\varepsilon_{xx}, \varepsilon_{yy}$	Normal strain components in shell in x and y directions, respectively
γ_{xy}, γ_{xz}, and γ_{yz}	Shear strain components in shell in xy, xz and yz planes, respectively
$\sigma_{xx}^{\text{shell}},\ \sigma_{yy}^{\text{shell}}$	Normal stress components in shell in x and y directions, respectively
$\tau_{xy}^{\text{shell}},\ \tau_{xz}^{\text{shell}}$ and τ_{yz}^{shell}	Shear stress components in shell in xy, xz and yz planes, respectively
$\sigma_{xx}^{stx},\ \sigma_{yy}^{sty}$	Normal stress components in stiffeners along x and y directions, respectively
N_{xx}, N_{yy}	Normal force resultants in x and y directions, respectively
N_{xy}, Q_{xz}, and Q_{yz}	Shear force resultants in xy, xz and yz planes, respectively
M_{xx}, M_{yy}	Normal moment resultants in x and y directions, respectively.
M_{xy}	Moment resultant in xy plane

ω	Natural frequency
ω_{nl}	Nonlinear natural frequency
q	Intensity of uniformly distributed pressure
Ω	Angular frequency of distributed pressure

Temperature-Dependent Material Properties of FGM

In the present study, any thermo-elastic material properties P (i.e., the modulus of elasticity E and the thermal expansion coefficient α) of the constituting materials (i.e., ceramic and metal)of the FGM are considered to be temperature-dependent and are evaluated by cubic fit equation of the form [38]:

$$P(T) = P_0\left(P_{-1}T^{-1} + 1 + P_1T + P_2T^2 + P_3T^3\right), \quad T \geq 300\,\mathrm{K}, \tag{1}$$

where P_0, P_{-1}, P_1, P_2 and $P_3$are material-specific constants and their values, given in Table 1, are evaluated experimentally [39].

It is assumed that the doubly-curved shallow shell is made up of FGM, a non-homogeneous combination of metal and ceramic, and the gradient of material properties is taken only in the thickness direction (i.e., z-direction). It is assumed that the top surface ($z = h/2$) is ceramic and the bottom one ($z = -h/2$) is metal surface.

It is to mention here that in the present study the Young's Modulus and thermal expansion coefficient of FGM shell are assumed to be temperature-dependent and calculated using the rule of the mixture as follows:

$$\begin{aligned} E_{\mathrm{eff}}(z,T) &= E_{\mathrm{c}}(T)V_{\mathrm{c}}(z) + E_{\mathrm{m}}(T)V_{\mathrm{m}}(z), \\ \alpha_{\mathrm{eff}}(z,T) &= \alpha_{\mathrm{c}}(T)V_{\mathrm{c}}(z) + \alpha_{\mathrm{m}}(T)V_{\mathrm{m}}(z). \end{aligned} \tag{2}$$

The material coefficients to evaluate these temperature-dependent material properties of the constituents of FGM i.e., $E_{\mathrm{c}}(T)$, $E_{\mathrm{m}}(T)$, $\alpha_{\mathrm{c}}(T)$ and $\alpha_{\mathrm{m}}(T)$ are given in Table 1.

The thermal conductivity $\kappa(z)$ and material density $\rho(z)$ of FGM are assumed to be temperature-independent and are calculated using:

$$\begin{aligned} \kappa(z) &= \kappa_{\mathrm{c}}V_{\mathrm{c}}(z) + \kappa_{\mathrm{m}}V_{\mathrm{m}}(z), \\ \rho(z) &= \rho_{\mathrm{c}}V_{\mathrm{c}}(z) + \rho_{\mathrm{m}}V_{\mathrm{m}}(z). \end{aligned} \tag{3}$$

The respective values of thermal conductivity of ceramic and metal are taken as $\kappa_{\mathrm{c}} = 1.0$ W/mK and $\kappa_{\mathrm{m}} = 1.7$ W/mK, respectively; whereas, the material density of ceramic and metal constituents are considered to be $\rho_{\mathrm{c}} = 3000$ kg/m^3 and $\rho_{\mathrm{m}} = 4429$ kg/m^3, respectively.

Further, in the Eqs. (2) and (3), V_{c} and V_{m} represent the volume fractions of ceramic and metal constituents of FGM shell, respectively, and are calculated across the shell-thickness as per the following power law:

$$V_{\mathrm{c}}(z) = \left(\frac{z}{h} + \frac{1}{2}\right)^k, V_{\mathrm{m}}(z) = 1 - V_{\mathrm{c}}(z) \text{ where } -h/2 \leq z \leq h/2. \tag{4}$$

where k is power law index which is used to control the FGM gradation profile and the subscripts 'c' and 'm' refer to the metallic and ceramic constituents of the FGM, respectively.

Based on the very small difference in the values of Poisson's ratio of the FGM constituents (i.e., ceramic and metal), the Poisson's ratio of the FGM is assumed to be the same as that of the constituents (i.e., 0.28) and it is taken to be constant across the thickness of FGM shell.

It is assumed that the temperature varies nonlinearly in the thickness direction, and its distribution is obtained by solving the following steady-state heat transfer equation:

$$-\frac{\mathrm{d}}{\mathrm{d}z}\left[\kappa(z)\frac{\mathrm{d}T}{\mathrm{d}z}\right] = 0, \quad T = T_{\mathrm{m}} \ \ at\ z = -h/2, \ \ T = T_{\mathrm{c}} \ \text{ at } z = h/2. \tag{5}$$

The aforementioned equation along with the boundary conditions can be solved by means of power series as [40]

$$T(z) = T_{\mathrm{m}} + \left(T_{\mathrm{c}} - T_{\mathrm{m}}\right)\lambda(z), \tag{6}$$

where,

$$\begin{aligned} \lambda(z) = \frac{1}{H}\Bigg[&\left(\frac{2z+h}{2h}\right) - \frac{\kappa_{\mathrm{cm}}}{(k+1)\kappa_{\mathrm{m}}}\left(\frac{2z+h}{2h}\right)^{k+1} \\ &- + \frac{\kappa_{\mathrm{cm}}^2}{(2k+1)\kappa_{\mathrm{m}}^2}\left(\frac{2z+h}{2h}\right)^{2k+1} \\ &- \frac{\kappa_{\mathrm{cm}}^3}{(3k+1)\kappa_{\mathrm{m}}^3}\left(\frac{2z+h}{2h}\right)^{3k+1} \\ &- + \frac{\kappa_{\mathrm{cm}}^4}{(4k+1)\kappa_{\mathrm{m}}^4}\left(\frac{2z+h}{2h}\right)^{4k+1} \\ &- \frac{\kappa_{\mathrm{cm}}^5}{(5k+1)\kappa_{\mathrm{m}}^5}\left(\frac{2z+h}{2h}\right)^{5k+1}\Bigg] \end{aligned} \tag{7}$$

Table 1 Material coefficients to evaluate temperature-dependent material properties of the constituents of FGM [38]

Material	Properties to be evaluated	Material coefficients				
		P_0	P_{-1}	P_1	P_2	P_3
ZrO_2	E (Pa)	244.27×10^9	0.0	-1.371×10^{-3}	1.214×10^{-6}	-3.681×10^{-10}
	α (1/K)	12.766×10^{-6}	0.0	-1.491×10^{-3}	1.006×10^{-5}	-6.778×10^{-11}
Ti–6Ali–4V	E (Pa)	122.56×10^9	0.0	-4.586×10^{-4}	0.0	0.0
	α (1/K)	7.5788×10^{-6}	0.0	6.638×10^{-4}	-3.147×10^{-6}	0.0

where, H and κ_{cm} are

$$H = 1 - \frac{\kappa_{\mathrm{cm}}}{(k+1)\kappa_{\mathrm{m}}} + \frac{\kappa_{\mathrm{cm}}^2}{(2k+1)\kappa_{\mathrm{m}}^2} - \frac{\kappa_{\mathrm{cm}}^3}{(3k+1)\kappa_{\mathrm{m}}^3} + \frac{\kappa_{\mathrm{cm}}^4}{(4k+1)\kappa_{\mathrm{m}}^4} - \frac{\kappa_{\mathrm{cm}}^5}{(5k+1)\kappa_{\mathrm{m}}^5}, \text{ and } \kappa_{\mathrm{cm}} = \kappa_{\mathrm{c}} - \kappa_{\mathrm{m}}.$$

Geometrical Model

A doubly curved shallow FGM shell possessing length, width and thickness as a, b and h, respectively, and having radii of curvature R_x and R_y along x-and y-directions is considered, as shown in Fig. 1. The Cartesian coordinate system, as shown in Fig. 1, is fixed at the mid-plane i.e., at $z=0$ of the shell. In the present analysis, generalized formulation is proposed for different types of shell geometries by setting the different combinations of curvatures as given in Table 2.

Stiffeners, as shown in Fig. 1, are used, along x and y direction, to reinforce the skin of the shell and are assumed to be made of the same isotropic and homogeneous material (ceramic or metal, as determined at $z = -h/2$ by the power law defined in Eq. 4) as that of the shell surface to avoid the material discontinuity. Geometrical parameters as presented in Fig. 1 for the stiffeners are defined as follows.

l_x and l_y are equal spacing between the stiffeners along x and y directions, respectively; e_x and e_y represent eccentricity of stiffeners along x and y directions, respectively, and they are defined as: $e_x=(h+h_x)/2$ and $e_y=(h+h_y)/2$, wherein h_x and h_y are the height of stiffeners in x and y directions, respectively; b_x and b_y denote the breadth of stiffeners along x and y directions, respectively, and; A_x and A_y stand for areas of cross section of stiffeners along x and y direction, respectively.

Table 2 Different curvatures to obtain different geometries of doubly-curved shell

Shell geometry	Principal curvatures of the shell	
	C_1	C_2
Plate	0	0
Cylindrical	$1/R_x$	0
Spherical	$1/R_x$	$1/R_y$
Hyperbolic-paraboloidal	$1/R_x$	$-1/R_y$

First-Order Shear Deformation Theory (FSDT)

According to the FSDT, the displacement components u, v, and w along x, y and z-direction, respectively, of an arbitrary point in the FGM shell can be evaluated using the corresponding displacement components u_0, v_0, w_0 at mid-surface of the shell (i.e., at $z=0$) and the slopes (ϕ_x, ϕ_y) of the transverse normal about the x- and y-axes, respectively, as follows [41]:

$$\begin{bmatrix} u(x,y,z,t) \\ v(x,y,z,t) \\ w(x,y,z,t) \end{bmatrix} = \begin{bmatrix} u_0(x,y,t) \\ v_0(x,y,t) \\ w_0(x,y,t) \end{bmatrix} + z \begin{bmatrix} \phi_x \\ \phi_y \\ 0 \end{bmatrix}. \tag{8}$$

Incorporating the geometrical nonlinearity in von Karman's sense (i.e., small strains and moderate rotations) in the FSDT, the strain components for doubly curved shallow shell can be written in the following form:

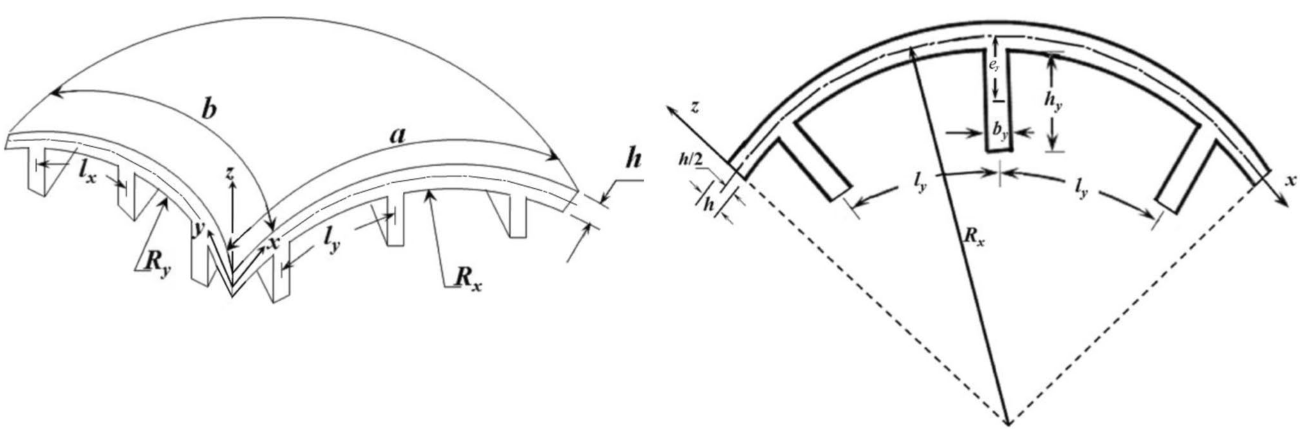

(a) (b)

Fig. 1 **a** Doubly curved shallow shell with stiffeners, and **b** geometry of FGM shallow shell with stiffeners in x–z plane

$$\begin{bmatrix} \varepsilon_{xx} \\ \varepsilon_{yy} \\ \gamma_{xy} \end{bmatrix} = \begin{bmatrix} \frac{\partial u_0}{\partial x} + C_1 w_0 + \frac{1}{2}\left(\frac{\partial w_0}{\partial x}\right)^2 \\ \frac{\partial v_0}{\partial y} + C_2 w_0 + \frac{1}{2}\left(\frac{\partial w_0}{\partial y}\right)^2 \\ \frac{\partial u_0}{\partial y} + \frac{\partial v_0}{\partial x} + \frac{\partial w_0}{\partial x}\frac{\partial w_0}{\partial y} \end{bmatrix} + z \begin{bmatrix} \frac{\partial \phi_x}{\partial x} \\ \frac{\partial \phi_y}{\partial y} \\ \frac{\partial \phi_x}{\partial y} + \frac{\partial \phi_y}{\partial x} \end{bmatrix} \tag{9}$$

and $\begin{bmatrix} \gamma_{xz} \\ \gamma_{yz} \end{bmatrix} = \begin{bmatrix} \phi_x + \frac{\partial w_0}{\partial x} - C_1 u_0 \\ \phi_y + \frac{\partial w_0}{\partial y} - C_2 v_0 \end{bmatrix}.$

Here, C_1 and C_2 are principal curvatures of the shell, as defined in Table 2.

The thermo-mechanical constitutive relations within the skin of the doubly-curved shallow shell can be expressed as:

$$\begin{Bmatrix} \sigma_{xx}^{\text{shell}} \\ \sigma_{yy}^{\text{shell}} \\ \tau_{yz}^{\text{shell}} \\ \tau_{xz}^{\text{shell}} \\ \tau_{xy}^{\text{shell}} \end{Bmatrix} = \begin{bmatrix} Q_{11} & Q_{12} & 0 & 0 & 0 \\ Q_{21} & Q_{22} & 0 & 0 & 0 \\ 0 & 0 & K_s Q_{44} & 0 & 0 \\ 0 & 0 & 0 & K_s Q_{55} & 0 \\ 0 & 0 & 0 & 0 & Q_{66} \end{bmatrix} \left[\begin{Bmatrix} \varepsilon_{xx} \\ \varepsilon_{yy} \\ \gamma_{yz} \\ \gamma_{xz} \\ \gamma_{xy} \end{Bmatrix} - \begin{Bmatrix} 1 \\ 1 \\ 0 \\ 0 \\ 0 \end{Bmatrix} \alpha(z, T)\Delta T(z, T) \right], \tag{10}$$

where, $Q_{11} = Q_{22} = \frac{E_{\text{eff}}(z,T)}{1-\nu^2}$, $Q_{12} = Q_{21} = \nu Q_{11}$, and $Q_{44} = Q_{55} = Q_{66} = \frac{E_{\text{eff}}(z,T)}{2(1+\nu)}$, K_s is the shear correction factor and its value is taken equal to 5/6 [42].

It is to mention that to consider the effect of temperature on the dynamic response of stiffened FGM shell, the top of FGM shell (i.e., ceramic side) is retained at elevated temperature whereas ambient temperature is assumed at the bottom of FGM shell (i.e., metallic side). The non-uniform temperature difference across the thickness is obtained using Eq. (6).

In the present study, the FGM shell is reinforced by rectangular stiffeners along both x and y directions and the contribution of stiffeners is considered based on smeared stiffener technique. As per this technique, if the stiffeners are placed closely and equally-spaced then the skin-stiffener interaction effect can be treated adequately by averaging the stiffening effects over the shell surface [43]. Moreover, it is assumed that the stiffeners are stressed uni-axially along their length only and hence, do not provide any shear resistance because of a large length-to-depth ratio. Further, the stiffeners are assumed to be perfectly connected to the shell and the normal strain components of stiffeners are similar to those of the shell. Based on the above assumptions, the relations between stress–strain for the stiffeners can be expressed as:

$$\left[\, \sigma_{xx}^{stx} \;\; \sigma_{yy}^{sty} \,\right] = E_0 \left[\, \varepsilon_{xx} \;\; \varepsilon_{yy} \,\right] \tag{11}$$

E_0 is the modulus of elasticity of material of the shell skin on which stiffeners are attached. The superscripts '*stx*' and '*sty*' are referring to the stiffeners in x and y directions, respectively.

The stress (both normal and shear) and moment resultants of the eccentrically stiffened shell can be expressed as:

$$\begin{bmatrix} N_{xx} \\ N_{yy} \\ N_{yy} \\ M_{xx} \\ M_{yy} \\ M_{xy} \end{bmatrix} = \int_{-h/2}^{h/2} \begin{bmatrix} \sigma_{xx}^{\text{shell}} \\ \sigma_{yy}^{\text{shell}} \\ \tau_{xy}^{\text{shell}} \\ z\sigma_{xx}^{\text{shell}} \\ z\sigma_{yy}^{\text{shell}} \\ z\tau_{xy}^{\text{shell}} \end{bmatrix} \mathrm{d}z + \begin{bmatrix} \frac{b_x}{l_x} \int_{e_x - h_x/2}^{e_x + h_x/2} \sigma_{xx}^{stx}\,\mathrm{d}z \\ \frac{b_y}{l_y} \int_{e_y - h_y/2}^{e_y + h_y/2} \sigma_{yy}^{sty}\,\mathrm{d}z \\ 0 \\ \frac{b_x}{l_x} \int_{e_x - h_x/2}^{e_x + h_x/2} z\sigma_{xx}^{stx}\,\mathrm{d}z \\ \frac{b_y}{l_y} \int_{e_y - h_y/2}^{e_y + h_y/2} z\sigma_{yy}^{sty}\,\mathrm{d}z \\ 0 \end{bmatrix} \text{ and } \begin{bmatrix} Q_{xz} \\ Q_{yz} \end{bmatrix} = \int_{-h/2}^{h/2} \begin{bmatrix} \tau_{xz} \\ \tau_{yz} \end{bmatrix} \mathrm{d}z \tag{12}$$

From Eqs. (9)–(12), the expressions for stress resultants in expanded forms can be written as:

$$N_{xx} = \left(A_{11} + \frac{E_0 A_x}{l_x}\right)\left\{\frac{\partial u_0}{\partial x} + C_1 w_0 + \frac{1}{2}\left(\frac{\partial w_0}{\partial x}\right)^2\right\} + \left(B_{11} + \frac{E_0 A_x e_x}{l_x}\right)\frac{\partial \phi_x}{\partial x} + A_{12}\left\{\frac{\partial v_0}{\partial y} + C_2 w_0 + \frac{1}{2}\left(\frac{\partial w_0}{\partial y}\right)^2\right\} + B_{12}\frac{\partial \phi_y}{\partial y}, \tag{13a}$$

$$N_{yy} = \left(A_{22} + \frac{E_0 A_y}{l_y}\right)\left\{\frac{\partial v_0}{\partial y} + C_2 w_0 + \frac{1}{2}\left(\frac{\partial w_0}{\partial y}\right)^2\right\} + \left(B_{22} + \frac{E_0 A_y e_y}{l_y}\right)\frac{\partial \phi_y}{\partial y} + A_{12}\left\{\frac{\partial u_0}{\partial x} + C_1 w_0 + \frac{1}{2}\left(\frac{\partial w_0}{\partial x}\right)^2\right\} + B_{12}\frac{\partial \phi_x}{\partial x} - N_y^T, \tag{13b}$$

$$N_{xy} = A_{66}\left(\frac{\partial u_0}{\partial y} + \frac{\partial v_0}{\partial x} + \frac{\partial w_0}{\partial x}\frac{\partial w_0}{\partial y}\right) + B_{66}\left(\frac{\partial \phi_x}{\partial y} + \frac{\partial \phi_y}{\partial x}\right), \tag{13c}$$

$$M_{xx} = \left(B_{11} + \frac{E_0 A_x e_x}{l_x}\right)\left\{\frac{\partial u_0}{\partial x} + C_1 w_0 + \frac{1}{2}\left(\frac{\partial w_0}{\partial x}\right)^2\right\} + \left(D_{11} + \frac{E_0 I_{xx}}{l_x} + \frac{E_0 A_x e_x^2}{l_x}\right)\frac{\partial \phi_x}{\partial x} + B_{12}\left\{\frac{\partial v_0}{\partial y} + C_2 w_0 + \frac{1}{2}\left(\frac{\partial w_0}{\partial y}\right)^2\right\} + D_{12}\frac{\partial \phi_y}{\partial y} - M_x^T, \tag{13d}$$

$$M_{yy} = \left(B_{22} + \frac{E_0 A_y e_y}{l_y}\right)\left\{\frac{\partial v_0}{\partial y} + C_2 w_0 + \frac{1}{2}\left(\frac{\partial w_0}{\partial y}\right)^2\right\} + \left(D_{22} + \frac{E_0 I_{yy}}{l_y} + \frac{E_0 A_y e_y^2}{l_y}\right)\frac{\partial \phi_y}{\partial y} + B_{12}\left\{\frac{\partial u_0}{\partial x} + C_1 w_0 + \frac{1}{2}\left(\frac{\partial w_0}{\partial x}\right)^2\right\} + D_{12}\frac{\partial \phi_x}{\partial x} - M_y^T, \tag{13e}$$

$$M_{xy} = B_{66}\left(\frac{\partial u_0}{\partial y} + \frac{\partial v_0}{\partial x} + \frac{\partial w_0}{\partial x}\frac{\partial w_0}{\partial y}\right) + D_{66}\left(\frac{\partial \phi_x}{\partial y} + \frac{\partial \phi_y}{\partial x}\right), \tag{13f}$$

$$Q_{xz} = K_s A_{55}\left(\phi_x + \frac{\partial w_0}{\partial x} - C_1 u_0\right) \text{ and } Q_{yz} = K_s A_{44}\left(\phi_y + \frac{\partial w_0}{\partial y} - C_2 v_0\right). \tag{13g}$$

where I_{xx} and I_{yy} are the area moment of inertia of stiffeners along x and y direction, respectively, and $\{A_{ij}, B_{ij}, D_{ij}\} = \int_{-h/2}^{h/2} \{1, z, z^2\} Q_{ij}\, \mathrm{d}z$ are the extensional, coupling and bending stiffnesses, respectively; and the thermal stress and moment resultants are defined as:

$$\begin{bmatrix} N_{xx}^T \\ N_{yy}^T \end{bmatrix} = \int_{-h/2}^{h/2} \begin{bmatrix} \frac{E_{\text{eff}}(z,T)}{1-\upsilon}\alpha_{\text{eff}}(z,\ T)\Delta T(z) \\ \frac{E_{\text{eff}}(z,T)}{1-\upsilon}\alpha_{\text{eff}}(z,\ T)\Delta T(z) \end{bmatrix} \mathrm{d}z; \text{ and } \begin{bmatrix} M_{xx}^T \\ M_{yy}^T \end{bmatrix} = \int_{-h/2}^{h/2} \begin{bmatrix} z\frac{E_{\text{eff}}(z,T)}{1-\upsilon}\alpha_{\text{eff}}(z,\ T)\Delta T(z) \\ z\frac{E_{\text{eff}}(z,T)}{1-\upsilon}\alpha_{\text{eff}}(z,\ T)\Delta T(z) \end{bmatrix} \mathrm{d}z. \tag{14}$$

To obtain the governing equations for vibration analysis of the FGM shell panels carrying stiffeners using variational approach under thermal environment, the total strain energy (U_{total}) and kinetic energy (K_{total}) of the system are written as:

$$\begin{aligned} U_{\text{total}} = \frac{1}{2}\int_V & \Big[\big(\sigma_{xx}^{(\text{shell})} + \sigma_{xx}^{stx}\big)\varepsilon_{xx} + \Big(\sigma_{yy}^{(\text{shell})} + \sigma_{yy}^{sty}\Big)\varepsilon_{yy} + \tau_{xy}\gamma_{xy} + \tau_{xz}\gamma_{xz} + \tau_{yz}\gamma_{yz} \\ & - \Big(\sigma_{xx}^{(\text{shell})} + \sigma_{yy}^{(\text{shell})}\Big)\alpha_{eff}(z,T)\Delta T(z,T)\Big]\,\mathrm{d}V \\ = \frac{1}{2}\int_A & \Big[\big(N_{xx} - N_x^T\big)\Big(u_{0,x} + C_1 w_0 + \frac{1}{2}w_{0,x}^2\Big) + \Big(N_{yy} - N_y^T\Big)\Big(v_{0,y} + C_2 w_0 + \frac{1}{2}w_{0,y}^2\Big) \\ & + N_{xy}\big(u_{0,y} + v_{0,x} + w_{0,x}w_{0,y}\big) + \big(M_{xx} - M_x^T\big)\phi_{x,x} + \Big(M_{yy} - M_y^T\Big)\phi_{y,y} \\ & + M_{xy}\big(\phi_{x,y} + \phi_{y,x}\big) + Q_{yz}\big(\phi_y + w_{0,y} - C_2 v_0\big) + Q_{yz}\big(\phi_x + w_{0,x} - C_1 u_0\big) + N^*\Big]\ \mathrm{d}A \end{aligned} \tag{15}$$

where, $N^* = \int_{-h/2}^{h/2} \frac{E_{\text{eff}}(z)}{(1-\upsilon)}\alpha_{eff}^2(z,T)\Delta T^2(z)\,\mathrm{d}z.$

For the total kinetic energy,

$$K_{\text{total}} = \frac{1}{2}\int_V \rho_{\text{eq}}(z)\big(\dot{u}^2 + \dot{v}^2 + \dot{w}^2\big)\mathrm{d}V = \frac{1}{2}\int_A \Big[I_0\big(\dot{u}_0^2 + \dot{v}_0^2 + \dot{w}_0^2\big) + I_1\big(\dot{u}_0\dot{\phi}_x + \dot{v}_0\dot{\phi}_y\big) + I_2\Big(\dot{\phi}_x^2 + \dot{\phi}_y^2\Big)\Big]\mathrm{d}A, \tag{16}$$

where, $(\cdot)$ indicates partial differentiation with respect to time (i.e., $\partial()/\partial t$).

$$\rho_{\text{eq}} = \rho(z) + \rho_0\left(\frac{A_x}{l_x h} + \frac{A_y}{l_y h}\right), \tag{17}$$

where $\rho_0 =$ the mass density of the material of stiffeners;

$$\text{and,}\ \ I_i = \int_{-h/2}^{h/2} \rho_{\text{eq}}(z) z^i \mathrm{d}z, \quad (i = 0,\ 1,\ 2). \tag{18}$$

In the present work, it is considered that the FGM shell is subjected to transverse harmonic distributed pressure (i.e., q), and the work done by this distributed pressure is written as:

$$W_q = \int_A q w_0\,\mathrm{d}A\,, \tag{19}$$

where $q = Q \sin \Omega t$, and Ω is the angular frequency of harmonic distributed pressure.

In the present study, the internal damping is assumed only in the transverse direction and the energy dissipated due to damping is given as [44]:

$$D = I_0\zeta \int_A w_0 \dot{w}_0\,\mathrm{d}A\,, \tag{20}$$

where is damping coefficient.

Governing Differential Equations

For nonlinear vibration analysis, the governing differential equations for FGM doubly curved shallow shell, with stiffeners and temperature gradient across the thickness, are derived by employing the extended Hamilton's principle for the non-conservative system with the following variational principle:

$$\int_0^t \big(\delta K_{\text{total}} - \delta U_{\text{total}} - \delta W_q - \delta D\big)\,\mathrm{d}t = 0. \tag{21}$$

Use integration-by-parts after inserting for U_{total}, K_{total}, W_q, and D from Eqs. (15), (16), (19), and (20), in Eq. (21), respectively; and then, collecting the coefficients of δu_0, δv_0, δw_0, $\delta\phi_x$ and $\delta\phi_y$ leads, respectively, to the following governing differential equations.

$$N_{x,x} + N_{xy,y} + C_1 Q_{xz} = I_0 \ddot{u}_0 + I_1 \ddot{\phi}_x, \tag{22a}$$

$$N_{y,y} + N_{xy,x} + C_2 Q_{yz} = I_0 \ddot{v}_0 + I_1 \ddot{\phi}_y, \tag{22b}$$

$$\begin{aligned} &Q_{xz,x} + Q_{yz,y} - C_1 N_x - C_2 N_y + N_x w_{0,xx} + N_{x,x} w_{0,x} + N_y w_{0,yy} + N_{y,y} w_{0,y} + 2N_{xy} w_{0,xy} \\ &+N_{xy,x} w_{0,y} + N_{xy,y} w_{0,x} + C_1 N_x^T + C_2 N_y^T - N_x^T w_{0,xx} - N_y^T w_{0,yy} + q = I_0 \ddot{w}_0 + 2\varsigma I_0 \dot{w}_0, \end{aligned} \tag{22c}$$

$$M_{x,x} + M_{xy,y} - Q_{xz} = I_1 \ddot{u}_0 + I_2 \ddot{\phi}_x, \tag{22d}$$

and $M_{y,y} + M_{xy,x} - Q_{yz} = I_1 \ddot{v}_0 + I_2 \ddot{\phi}_y.$ (22e)

Further, using Eqs. 13(a)–(g), Eqs. 22(a)–(e) are expanded in the following forms:

$$l_{11}(u_0) + l_{12}(v_0) + l_{13}(w_0) + l_{14}(\phi_x) + l_{15}(\phi_y) + n_1(w_0^2) = I_0 \ddot{u}_0 + I_1 \ddot{\phi}_x, \tag{23a}$$

$$l_{21}(u_0) + l_{22}(v_0) + l_{23}(w_0) + l_{24}(\phi_x) + l_{25}(\phi_y) + n_2(w_0^2) = I_0 \ddot{v}_0 + I_1 \ddot{\phi}_y, \tag{23b}$$

$$\begin{aligned} &l_{31}(u_0) + l_{32}(v_0) + l_{33}(w_0) + l_{34}(\phi_x) + l_{35}(\phi_y) + n_3(w_0^2) + n_4(w_0^3) + n_5(u_0 w_0) \\ &+n_6(v_0 w_0) + n_7(w_0 \phi_x) + n_8(w_0 \phi_y) - q = I_0 \ddot{w}_0 + 2\zeta I_0 \dot{w}_0, \end{aligned} \tag{23c}$$

$$l_{41}(u_0) + l_{42}(v_0) + l_{43}(w_0) + l_{44}(\phi_x) + l_{45}(\phi_y) + n_9(w_0^2) = I_1 \ddot{u}_0 + I_2 \ddot{\phi}_x, \tag{23d}$$

$$l_{51}(u_0) + l_{52}(v_0) + l_{53}(w_0) + l_{54}(\phi_x) + l_{55}(\phi_y) + n_{10}(w_0^2) = I_1 \ddot{v}_0 + I_2 \ddot{\phi}_y, \tag{23e}$$

where, all linear and nonlinear operators in the set of governing differential equations Eq. (21) are represented, respectively, by l_{ij} () and n_i () symbols and, are presented in expanded form in "Appendix A".

Solution Methodology

The present study explores the nonlinear dynamic behavior of simply-supported FGM shallow shell, the boundary conditions at different edges of the shell are defined as:

$$\begin{aligned} &v_0 = w_0 = \phi_y = 0,\ M_x = N_x = N_{xy} = 0 \text{ at } x = 0 \text{ and } x = a, \\ &u_0 = w_0 = \phi_x = 0,\ M_y = N_y = N_{xy} = 0 \text{ at } y = 0 \text{ and } y = b. \end{aligned} \tag{24}$$

Assuming the Navier solutions for the simply-supported FGM shell, the following admissible trigonometric displacement and rotation functions, satisfying the above-mentioned boundary conditions in Eq. (22), are introduced in the aforementioned set of governing differential equations [i.e., Eqs. 21(a)-(e)].

$$\begin{aligned} &u_0 = U(t)\cos\frac{m\pi x}{a}\sin\frac{n\pi y}{b},\ v_0 = V(t)\sin\frac{m\pi x}{a}\cos\frac{n\pi y}{b}, \\ &w_0 = W(t)\sin\frac{m\pi x}{a}\sin\frac{n\pi y}{b}, \\ &\phi_x = X(t)\cos\frac{m\pi x}{a}\sin\frac{n\pi y}{b},\ \phi_y = Y(t)sin\frac{m\pi x}{a}\cos\frac{n\pi y}{b}. \end{aligned} \tag{25}$$

It is to mention that U, V, W, X, and Y are the vibration amplitudes in the corresponding directions, whereas m and n are half wave numbers along x and y directions, respectively.

By substituting the assumed admissible displacement and rotation functions from Eq. (25) into Eqs. 23(a)–(e), and applying the Galerkin method over the shell domain, the partial differential equations [i.e., Eqs. 23(a)–(e)] are converted into the following nonlinear governing equations.

$$C_{11}U + C_{12}V + C_{13}W + C_{14}X + C_{15}Y + N_1 W^2 = I_0 \ddot{U} + I_1 \ddot{X}, \tag{26a}$$

$$C_{21}U + C_{22}V + C_{23}W + C_{24}X + C_{25}Y + N_2 W^2 = I_0 \ddot{V} + I_1 \ddot{Y}, \tag{26b}$$

Table 3 Verification of non-dimensional natural frequency $\bar{\omega} = \omega h\sqrt{\rho_c/E_c}$.

	$k=0$	$k=1$	$k=4$	$k=10$
Plate ($C_1 = C_2 = 0$)				
Present study	0.0577	0.0441	0.0384	0.0358
Wattanasakulpong and Chaikittiratana [22]	0.0577	0.0442	0.0382	0.0366
Matsunaga [45]	0.0577	0.0443	0.0381	0.0364
Cylindrical Panel $\left(C_1 = 0.5,\ C_2 = 0\right)$				
Present study	0.0623	0.0487	0.0400	0.0385
Wattanasakulpong and Chaikittiratana [22]	0.0617	0.0477	0.0407	0.0385
Matsunaga [45]	0.0622	0.0485	0.0413	0.0390
Alijani et al. [28]	0.0615	0.0476	-	0.0383
Spherical Panel $\left(C_1 = C_2 = 0.5\right)$				
Present study	0.0820	0.0604	0.0489	0.0468
Wattanasakulpong and Chaikittiratana [22]	0.0746	0.0588	0.0491	0.0455
Matsunaga [45]	0.0751	0.0600	0.0503	0.0464
Alijani et al. [28]	0.0746	0.0589	-	0.0455
Hyperbolic-paraboloidal panel $\left(C_1 = 0.5,\ C_2 = -0.5\right)$				
Present study	0.0565	0.0441	0.0384	0.0358
Wattanasakulpong and Chaikittiratana [22]	0.0548	0.0420	0.0363	0.0347
Matsunaga [45]	0.0563	0.0432	0.0372	0.0355

Table 4 Verification of non-dimensional natural frequency $\bar{\omega} = \left(\omega a^2/h\right)\sqrt{\left(1-\nu^2\right)\rho_m/E_m}$ of square FGM plate with $h/a = 0.125$ and $a/b = 1$ under thermal environment

	$k=0$	$k=0.5$	$k=1$	$k=2$
$T_m=300$ K, $T_c=300$ K				
Present study	12.609	8.916	7.638	6.846
Alijani et al. [46]	12.528	8.622	7.557	6.786
Huang and Shen [47]	12.495	8.675	7.555	6.777
$T_m=300$ K, $T_c=400$ K				
Present study	12.576	8.635	7.565	6.9836
Alijani et al. [46]	12.332	8.468	7.414	6.649
Huang and Shen [47]	12.397	8.615	7.474	6.693
$T_m=300$ K, $T_c=600$ K				
Present study	12.001	8.581	7.398	6.785
Alijani et al. [46]	11.919	8.138	7.102	6.346
Huang and Shen [47]	11.984	8.269	7.171	6.398

$$C_{41}U + C_{42}V + C_{43}W + C_{44}X + C_{45}Y + N_9\,W^2 = I_1\ddot{U} + I_2\ddot{X}, \tag{26d}$$

$$C_{51}U + C_{52}V + C_{53}W + C_{54}X + C_{55}Y + N_{10}W^2 = I_1\ddot{V} + I_2\ddot{Y}, \tag{26e}$$

In the Eqs. 26(a)–(e), the C_{ij} $(i, j=1, 2,\ldots 5)$ and N_i $(i=1, 2, \ldots 10)$ represent the coefficients of linear and nonlinear terms, respectively, and the same are specified in "Appendix B".

The natural frequencies are calculated by solving the standard eigen value problem formulated by ignoring the nonlinear and damping terms and setting $q=0$ in the Eqs. 226(a)–(e). Thereafter, the dynamic response of doubly-curved shallow FGM shells reinforced with stiffeners can be determined by solving time-dependent nonlinear governing equations Eqs. 26(a)–(e) using the fourth order Runge–Kutta method, along with the initial conditions:

$$\begin{aligned} &C_{31}U + C_{32}V + C_{33}W + C_{34}X + C_{35}Y + N_3W^2 + N_4W^3 + N_5UW + N_6VW \\ &+N_7WX + N_8WY - \frac{16q}{\pi^2 mn} = I_0\ddot{W} + 2\zeta I_0\dot{W}, \end{aligned} \tag{26c}$$

Table 5 Comparison of non-dimensional natural frequency of Al_2O_3/Al FGM spherical shell panels with $a/b=1.0$, $a/h=20$, $h_x=h_y=3\,h$, and $h_x/b_x=h_y/b_y=5.0$

Power law index (k)	0	2	4	6	8	10
Present work	2.337	1.997	1.892	1.838	1.799	1.761
Wattanasakulpong and Chaikittiratana [22]	2.456	2.113	2.002	1.945	1.907	1.869

Table 6 Comparison of non-dimensional natural frequency of Si_3N_4/SUS304 FGM spherical shell panels under thermal environment with $a/b=1.0$; $a/h=20$, $k=0.5$, $h_x=h_y=3\,h$, $h_x/b_x=h_y/b_y=5.0$

a/R_x	0.5	1	1.5	2	2.5	3
Present work	1.912	2.217	2.666	2.978	3.232	3.439
Wattanasakulpong and Chaikittiratana [22]	1.679	1.934	2.330	2.755	3.142	3.443

Table 7 Comparison of nonlinear-linear frequency ratios (ω_{nl}/ω) of simply-supported cylindrical shell panel of FGM Si_3N_4/SUS304 (for $k=2$ and $a/h=20$)

$\bar{W}$	$aC_1=1/5$		$aC_1=1/2$	
	Present work	Shen and Wang [30]	Present work	Shen and Wang [30]
0.20	1.021	1.020	1.009	1.012
0.40	1.087	1.069	1.043	1.045
0.60	1.193	1.149	1.106	1.100
0.80	1.330	1.253	1.198	1.173
1.00	1.487	1.373	1.313	1.259

$$U(0)=V(0)=W(0)=X(0)=Y(0)=0\,;$$

and

$$\dot{U}(0)=\dot{V}(0)=\dot{W}(0)=\dot{X}(0)=\dot{Y}(0)=0. \tag{27}$$

Numerical Studies and Discussion

To carry out the present research work, a MATLAB code based on the generalized analytical formulation for different shell configurations was developed for conducting linear and nonlinear vibration analysis of unstiffened- and stiffened- FGM doubly-curved shallow shells. The accuracy of developed code is established through various verification studies conducted by comparing the results obtained with those reported in the literature. After the verification studies, a parametric study was conducted to investigate the linear and nonlinear dynamic behavior of un-stiffened and stiffened doubly-curved shallow Ti–6Al–4V/ZrO_2 FGM shells with temperature-dependent material properties, as given in Table 1. Numerical results are presented for free and forced vibration analysis of different shell geometries obtained by setting the different combinations of curvatures, as given in Table 2.

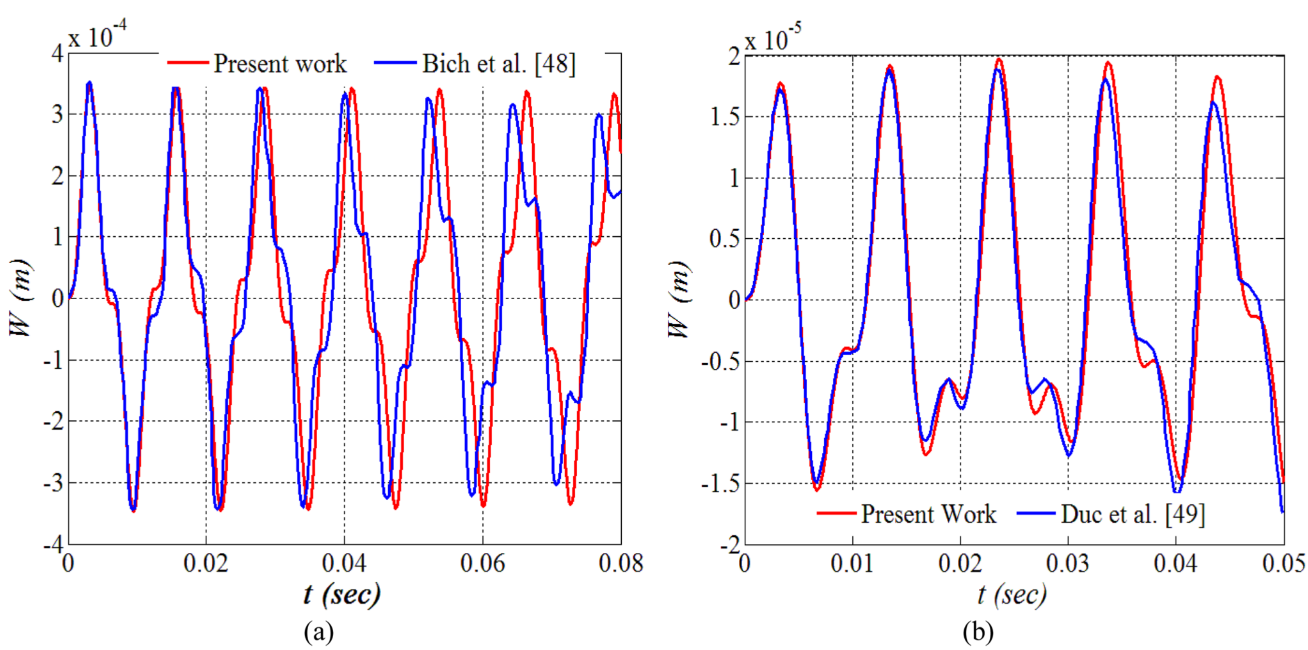

Fig. 2 Comparison of nonlinear vibration response of **a** stiffened FGM spherical panel for $k=1$, $a/b=1$, $a/h=30$, $m=n=1$, $R_x=R_y=6$ m, $=\xi$ 0.1, $q=5000$ sin (500t), and **b** FGM plate for $k=1$, $a/b=1$, $a/h=20$, $m=n=1$, $=0.1$, $q=1500$ sin (600t) and $T=105$ K

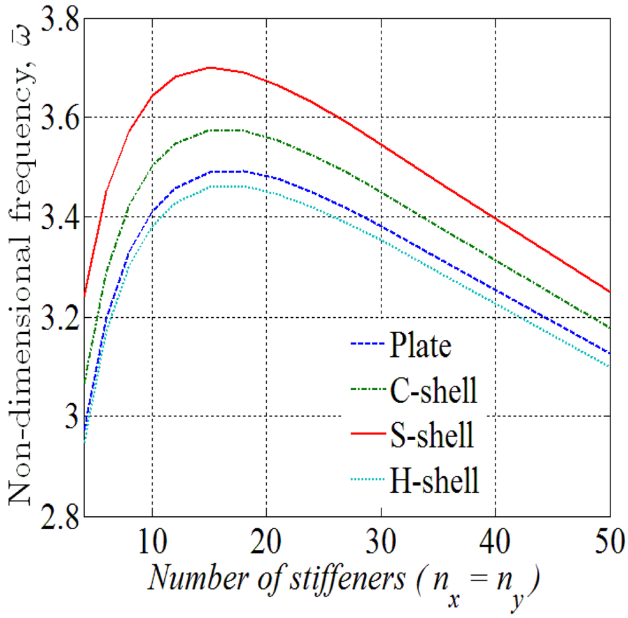

Fig. 3 Effect of the number of stiffeners on non-dimensional natural frequency ($\bar{\omega}$) of stiffened FGM (ZrO_2/Ti–6Al–4V) shell panels with different geometries ($k=1$)

Table 8 Non-dimensional natural frequency ($\bar{\omega}$) of un-stiffened and stiffened FGM (ZrO_2/Ti–6Al–4V) doubly-curved shallow shells ($n_x = n_y = 15$, and $\Delta T = 0$ K)

Shell type	Power law index	Un-stiffened	Stiffened
Plate	0	2.1635	5.0210
	0.5	1.8572	3.6105
	1	1.7395	3.5115
	5	1.5597	3.3438
	∞	1.4851	3.3013
Cylindrical shell panel	0	2.2779	5.1387
	0.5	1.9571	3.7024
	1	1.8320	3.5993
	5	1.6372	3.4237
	∞	1.5598	3.3791
Spherical shell panel	0	2.6055	5.3070
	0.5	2.2438	3.8387
	1	2.0982	3.7287
	5	1.8622	3.5395
	∞	1.7755	3.4910
Hyperbolic-paraboloidal shell panel	0	2.1459	4.9775
	0.5	1.8421	3.5794
	1	1.7253	3.4813
	5	1.5470	3.3149
	∞	1.4730	3.2727

Verification Studies

In the first verification study, non-dimensional natural frequencies ($\bar{\omega} = \omega h\sqrt{\rho_c/E_c}$ of un-stiffened, doubly-curved FGM shallow shells (with $a/b=1$, $a/h=10$) of different geometrical configurations (i.e., plate, cylindrical, spherical, and hyperbolic-paraboloidal) and different power law index (i.e., 0, 1, 4, 10) are compared with the results reported in the literature by Wattanasakulpong and Chaikittiratana [22], Alijani et al. [28], and Matsunaga [45]. The FGM shell panels were assumed to be simply-supported and made up of Al/Al_2O_3 with temperature-independent material properties (i.e., $E_m = 70\times10^9$ N/m^2, $\rho_m = 2702$ kg/m^3, $E_c = 380\times10^9$ N/m^2 and $\rho_c = 3800$ kg/m^3). Table 3 shows the comparison of results, and it can be observed from this table that the results obtained from the present formulation are in good concurrence with the results published in the literature.

In the second verification study, the non-dimensional natural frequency $\bar{\omega} = \left(\omega a^2/h\right)\sqrt{\left(1-\nu^2\right)\rho_m/E_m}$ of an unstiffened SUS304/Si_3N_4 FGM plate (i.e., $(C_1 = C_2 = 0)$) with simply-supported boundary condition is compared with that reported by Alijani [46] and Huang and Shen [47], for different power law index (i.e., 0, 0.5, 1, 2) and for different values of temperature differences (i.e., $\Delta T = 0$ K, 100 K, 300 K). The material properties were considered to be temperature-dependent. The results are tabulated in Table 4. It can be ascertained from Table 4 that the present results are in good compliance with the published results by Alijani [46] and Huang and Shen [47].

In addition, the non-dimensional natural frequency $\left(\bar{\omega} = 10^2\omega h\sqrt{\rho_{0c}/E_{0c}}\right)$ of Al_2O_3/Al and Si_3N_4/SUS304 FGM spherical shell panels containing 10 stiffeners in x and y directions both were compared with the values presented by Wattanasakulpong and Chaikittiratana [22]. The results of comparison for spherical shell panels made of Al_2O_3/Al are shown in Table 5 for different power law index; whereas, for Si_3N_4/SUS304 FGM with temperature-dependent material properties under thermal environment (i.e., $\Delta T = 100$ K), the results are presented in Table 6 for different values of side-to-radius of curvature ratio (i.e., a/R_x). An acceptable agreement between the results of current study and the literature can be seen in Table 5 and Table 6.

Furthermore, to verify the nonlinear formulation, the nonlinear frequency ratio ω_{nl}/ω for a simply-supported Si_3N_4/SUS304 FGM cylindrical shell panel obtained using the present formulation is compared with the results reported by Shen and Wang [30]. As evident from Table 7, the results of the present formulation are in good accordance with the literature [30]. However, a little difference in the values in Table 7 can be ascribed to the use of different deformation theories- higher-order shear deformation theory by Shen and

Table 9 Effect of the temperature difference across thickness on the non-dimensional natural frequency ($\bar{\omega}$) of FGM (ZrO_2/Ti–6Al–4V) doubly-curved shallow shells ($n_x = n_y = 15$)

Shell type	Power law index	$\Delta T = 0$ K	$\Delta T = 100$ K	$\Delta T = 300$ K
Plate	0	5.0210	4.7371	4.2280
	0.5	3.6105	3.5394	3.3546
	1	3.5115	3.4567	3.3107
	5	3.3438	3.3212	3.2604
	∞	3.3013	3.2909	3.2562
Cylindrical shell panel	0	5.1387	4.8502	4.3385
	0.5	3.7024	3.6298	3.4455
	1	3.5993	3.5435	3.3983
	5	3.4237	3.4010	3.3411
	∞	3.3791	3.3690	3.3350
Spherical shell panel	0	5.3070	5.0117	4.4946
	0.5	3.8387	3.7647	3.5880
	1	3.7287	3.6724	3.5347
	5	3.5395	3.5170	3.4599
	∞	3.4910	3.4777	3.4491
Hyperbolic-paraboloidal shell panel	0	4.9775	4.6957	4.1899
	0.5	3.5794	3.5087	3.3244
	1	3.4813	3.4267	3.2811
	5	3.3149	3.2923	3.2317
	∞	3.2727	3.2624	3.2277

Wang [30], and first-order shear deformation theory in the present work.

Additionally, the accuracy of the present formulation in predicting the nonlinear vibration response of stiffened FGM structures is established by comparing the nonlinear vibration response of Al/Al_2O_3 FGM stiffened spherical shell panel subjected to uniformly distributed pressure with Bich et al. [48], as shown in Fig. 2a. While Fig. 2b depicts a similar comparison of nonlinear vibration response of Al/Al_2O_3 FGM stiffened plate under thermal environment (i.e., $\Delta T = 105^0$ K) with Duc et al. [49]. The comparisons shown in Fig. 2a, b assure the reliability of the present formulation in predicting the nonlinear vibration response of FGM stiffened shell panels under mechanical as well as thermal loadings.

Parametric Investigation and Discussion

After verification of the present formulation, a parametric study is conducted to explore the linear and nonlinear dynamic behavior of un-stiffened and stiffened doubly curved shallow Ti–6Al–4V/ZrO_2 FGM shells with temperature-dependent material properties, as given in Table 1. It is important to mention here that all the numerical studies are conducted by considering: half-wave numbers $m = n = 1$, aspect ratio, $a/b = 1$, and $a/h = 20$ with different shell geometries obtained by setting $C_1 = C_2 = 0$ for plate, $C_1 = 1/5$, $C_2 = 0$ for cylindrical, $C_1 = C_2 = 1/5$ for spherical, and $C_1 = 1/5$, $C_2 = -1/5$ for hyperbolic-paraboloidal shell panels, as mentioned in Table 2. Moreover, for stiffened shell panels the heights (i.e., $h_x = h_y$) and widths (i.e., $b_x = b_y$) of the stiffeners are taken as 3 h and 3 $h/10$ respectively, where h being the thickness of the shell. In addition, the natural frequency is presented in the non-dimensional form as: $\bar{\omega} = 10^2 \omega h \sqrt{\rho_m (1 - \upsilon^2) / E_m}$.

In order to fix the number of stiffeners (i.e., n_x, n_y), the effect of number of stiffeners (with $n_x = n_y$) on non-dimensional natural frequency (i.e., $\bar{\omega} = 10^2 \omega h \sqrt{\rho s (1 - \upsilon^2) / E_m}$) of the FGM plate and three different FGM (with $k = 1$) stiffened shell geometries was studied and the plots obtained are shown in Fig. 3. It is found that initially with the increase in the number of stiffeners, the natural frequency increases up to 15 stiffeners and thereafter, the natural frequency decreases. This is true for the plate as well as for other considered shell geometries. It can also be observed from Fig. 3 that irrespective of the number of equal stiffeners in x and y directions, spherical shell has the highest natural frequency, whereas the hyperbolic-paraboloidal shell is found to have a lowest natural frequency. Based on the finding that the effect of 15 stiffeners ($n_x = n_y = 15$) is most significant on the natural frequency, it is to mention here that in any of the subsequent investigations on stiffened shell panels, the number of stiffeners in x- and y-directions both is taken equal to 15.

Table 8 shows the effect of stiffeners on the non-dimensional natural frequencies ($\bar{\omega}$) of free vibration of FGM shell panels of different geometries, for different values of power law index. It can be seen that the non-dimensional natural frequency ($\bar{\omega}$) of stiffened shell panels are significantly greater than that of unstiffened ones. It can also be observed that natural frequency decreases with the increase of power law index, k and the effect of stiffeners is more prominent for power law index, $k = 0$ (i.e., ceramic) than other values of k. This is because of the reason that for $k = 0$, the whole panel, including the stiffeners, would be made of ceramic material.

Table 9 illustrates the effect of the temperature difference (i.e., $\Delta T = 0$ K, 100 K, 300 K) across the thickness of stiffened FGM shell panels of different geometries on the non-dimensional natural frequency, for different values of power law index, k. It can be clearly seen from Table 9 that a higher temperature difference will lower the non-dimensional natural frequency remarkably. In addition, it can also be observed from Tables 8 and 9 that the natural frequencies of spherical and hyperbolic-paraboloidal shell panels are highest and lowest, respectively, among all the shell geometries considered in the present work.

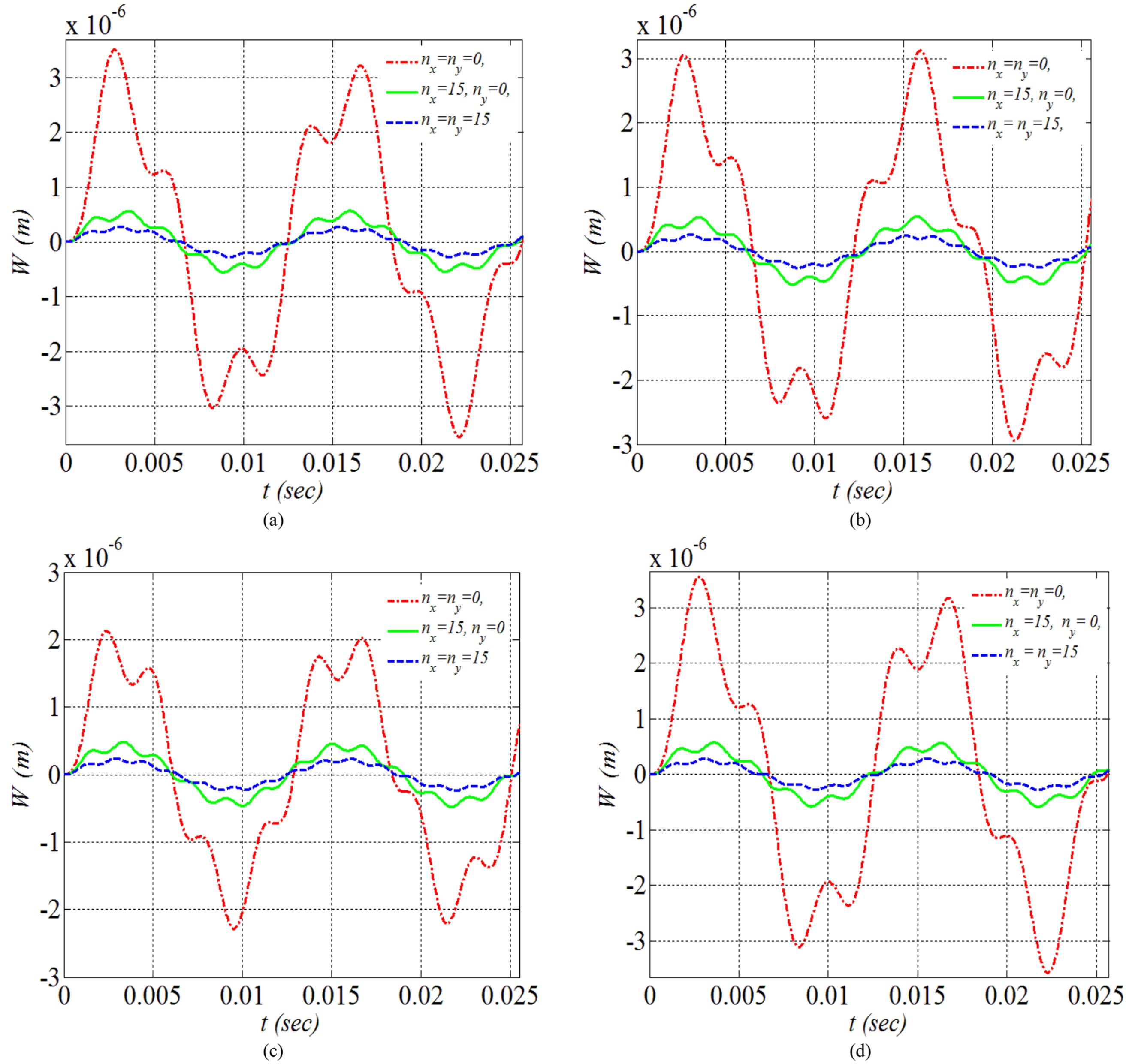

Fig. 4 Nonlinear vibration response of FGM **a** plate **b** cylindrical, **c** spherical, and **d** hyperbolic-paraboloidal shell panels with and without stiffeners (for $k=1$ and $q=1500\sin(600t)$)

Figure 4a–d present comparisons of the amplitude of nonlinear dynamic response of un-stiffened and stiffened (i.e., uni-directional stiffened and orthogonally stiffened) shell panels of different shell geometries. It is quite evident from these Figs that irrespective of shell geometry, shell panels without stiffeners show a considerably large amplitude of nonlinear forced vibration in comparison to uni-directional stiffened and orthogonally stiffened shell panels. This is attributed to the reason that shell panels without stiffeners have lower stiffness.

Figure 5 (a-d) depicts the effect of FGM power law index on the nonlinear dynamic response of the stiffened shells panels of different geometries under a harmonic force of constant amplitude. A similar study is shown in Fig. 6a–d at resonance condition (i.e., $\Omega/\omega=1$). It can be clearly seen in Figs. 5a–d and 6a–d that with the increase of power law index, value of the maximum amplitude of nonlinear vibration of stiffened shell panels increases. This can be attributed to the fact that with the increase of power law index, metal (having lower stiffness than ceramic) proportion is increased

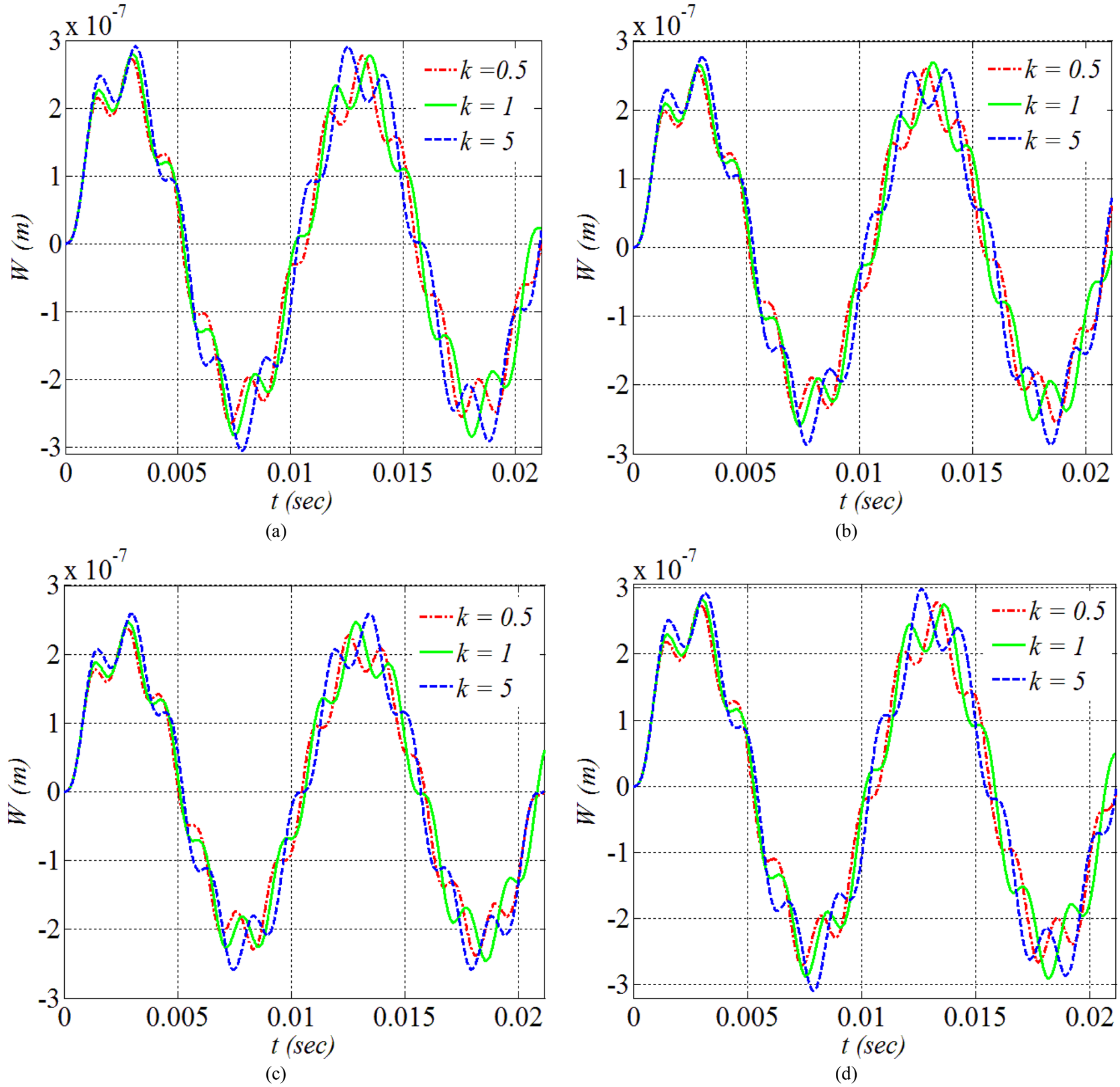

Fig. 5 Nonlinear vibration response of FGM **a** plate **b** cylindrical, **c** spherical, and **d** hyperbolic -paraboloidal shell panels (for $n_x = n_y = 15$ and $q = 1500\sin(600t)$)

in FGM causing a decrease in the overall stiffness of the FGM panel, and hence, the amplitude of vibration increases. It is justifiable to mention that with the increase in power law index natural frequency decreases and it can be seen clearly in the case of resonance in Figs. 6 (a-d) that the time period of vibration response increases significantly.

Effect of the temperature difference on nonlinear dynamic responses of the stiffened shell panels at different excitation frequencies (i.e., $\Omega = 600$ and $\Omega/\omega = 0.95$) is shown, respectively, in Figs. 7a–d and 8a–d. To achieve the temperature difference, the metal surface is kept at a temperature (T_m) of 300 K while the ceramic surface temperature (T_c) is taken as 300 K, 400 K and 600 K. As observed from Fig. 7a–d that temperature difference rise results in the increase of vibration amplitude, for all geometries of shell panels. Further, as demonstrated in Fig. 8a–d, the rise in temperature difference across the thickness of FGM shell panels also results in an increase in the time period of the beat phenomenon, a vibrational behaviour of engineering structures observed when the excitation frequency is close

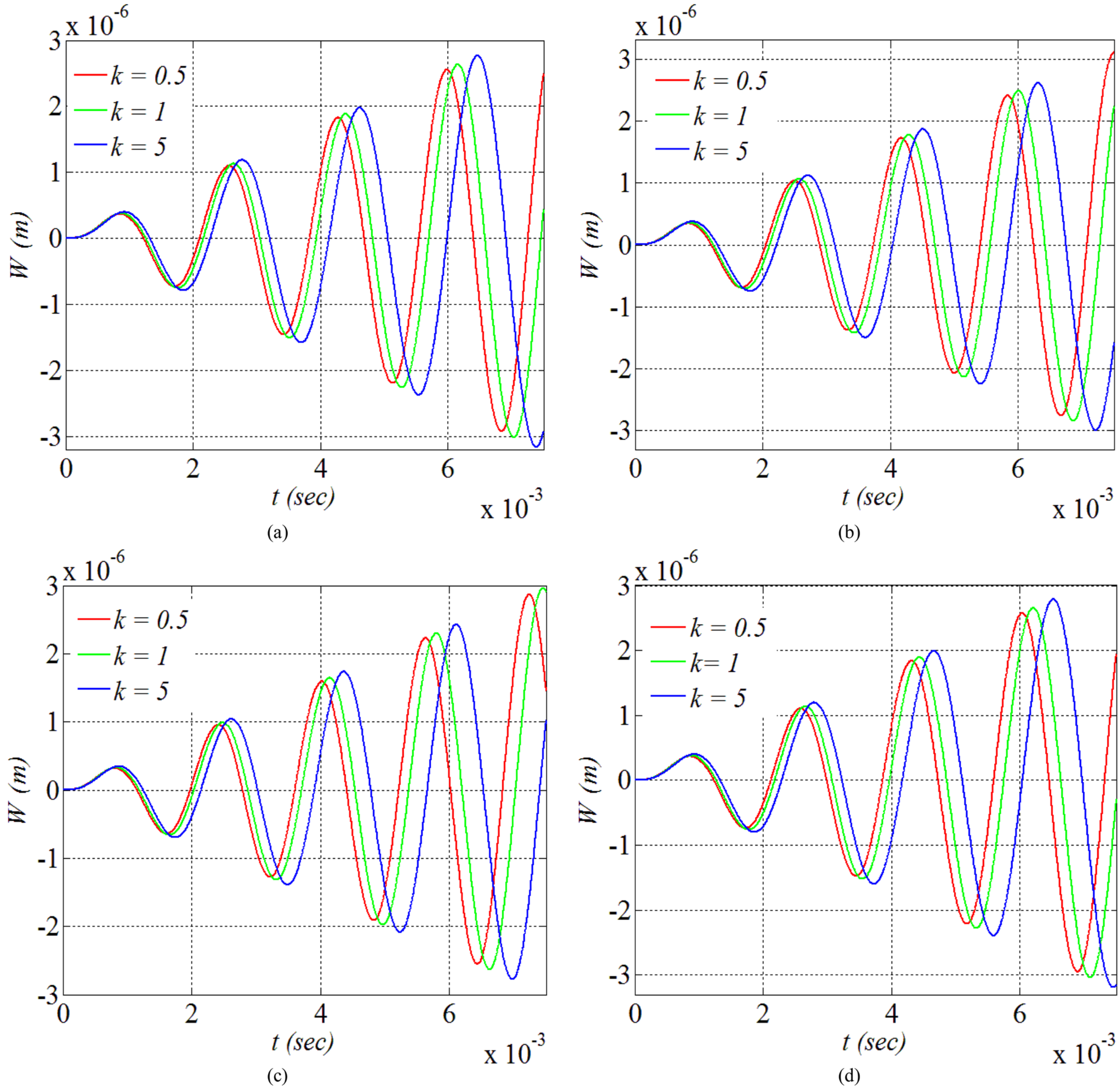

Fig. 6 Nonlinear vibration response of FGM (**a** plate **b** cylindrical, **c** spherical, and **d** hyperbolic -paraboloidal shell panels at different values of power law index k (for $q = 1500\sin(\Omega t)$ with $\Omega/\omega = 1, \xi = 0$, and $n_x = n_y = 15$)

to the natural frequency. These observations are customary because an increase in the temperature difference across the thickness reduces the stiffness of the shell panels.

The effect of damping on the nonlinear vibration response of a typical stiffened spherical FGM shell panel is studied here. Figure 9 shows the effect of damping on nonlinear vibration response the spherical FGM shell panel but in the absence of excitation force. The initial conditions were taken as: $W = 10^{-7}\ m$ and $\dot{W} = 0$. It can be observed that the amplitude of vibration reduces exponentially with time. Further, the effect of damping under the condition of resonance (i.e., $\Omega/\omega = 1$) shown in Fig. 10 demonstrates that initially the impact of damping is indistinguishable and thereafter, a substantial difference in the amplitude caused by damping can be observed after a few initial periods of vibration. It is also observed from Fig. 10 that the amplitude of undamped nonlinear vibration response increases linearly in an unbounded manner with time, whereas the

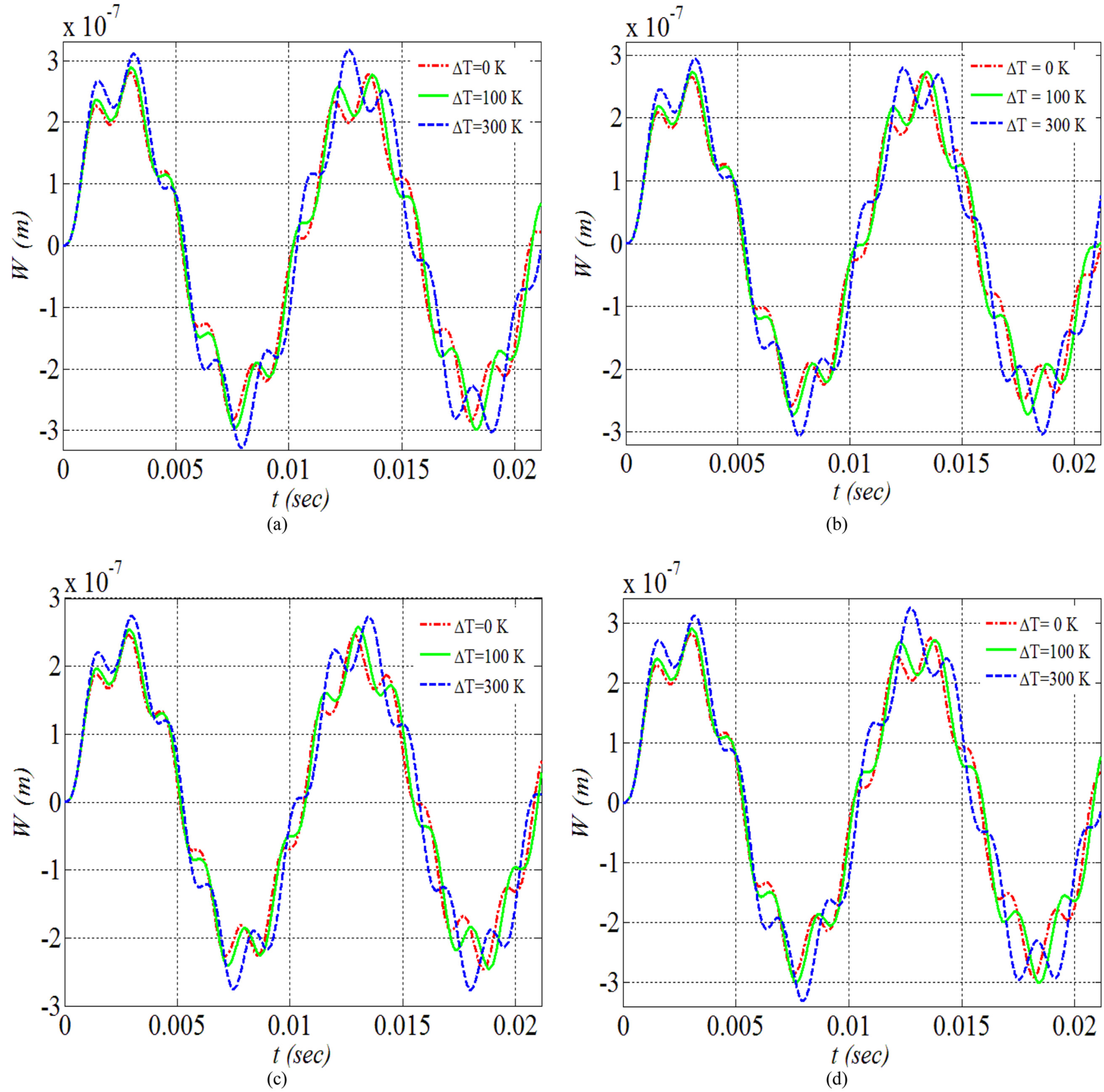

Fig. 7 Nonlinear vibration response of FGM **a** plate, **b** cylindrical, **c** spherical, and **d** hyperbolic-paraboloidal shell panels under different temperature differences ΔT across thickness (for $k=1$, $n_x=n_y=15$, and $q=1500\sin(600t)$)

amplitude of damped nonlinear vibration response is bounded and it reduces considerably in comparison to undamped nonlinear vibration response. Further, Fig. 11 shows that the effect of damping is not clearly observable during the time periods of the first few beats, but the effect in terms of reduction in the amplitude is apparent thereafter in successive time periods.

Conclusion

In the present paper, an analytical formulation based on the first-order shear deformation theory in conjunction with von Karman geometric nonlinearity is utilized for the dynamic analysis of eccentrically stiffened, simply-supported doubly-curved FGM shallow shell panels under thermo-mechanical

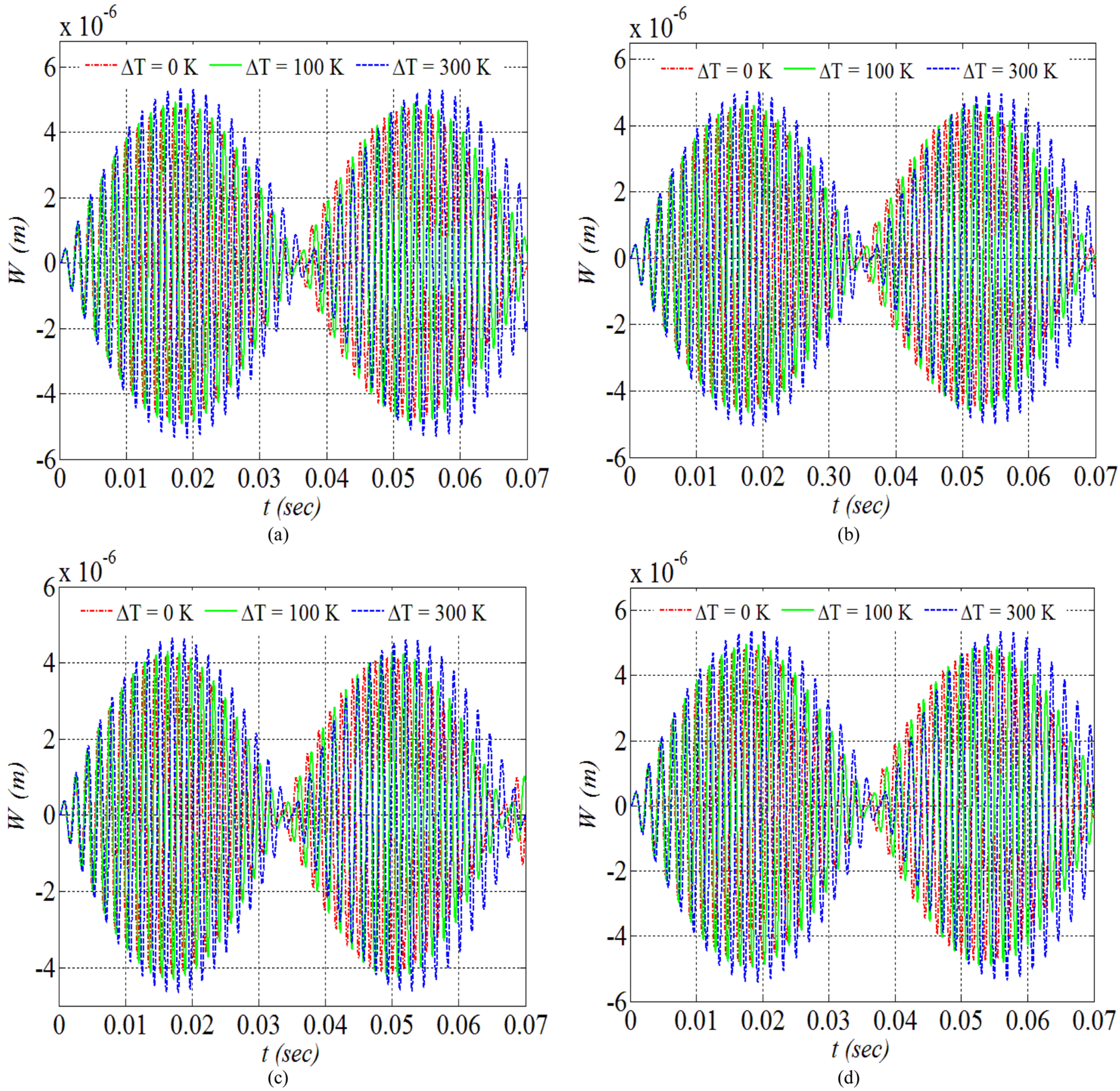

Fig. 8 Nonlinear vibration response (i.e., beat phenomenon) of FGM **a** plate, **b** cylindrical, **c** spherical, and **d** hyperbolic -paraboloidal shell panels under different temperature differences ΔT across thickness (for $q = 1500\sin(\Omega t)$ with $\Omega / \omega = 0.95$, $\xi = 0$, $k = 1$, and $n_x = n_y = 15$)

loading. After ascertaining the accuracy of the formulation by comparing the results obtained, for FGM (with temperature-dependent and –independent material properties) shell panels of different geometries, in the present study with the published results in the literature, a parametric study is conducted to investigate the effect of shell geometries, stiffeners, material inhomogeneity, different temperature differences across the thickness, and material parameters on the natural frequency, and nonlinear dynamic response. Natural frequencies are obtained by solving a linear standard eigenvalue problem. Galerkin method is used to obtain the coupled differential equations of motion with cubic and quadratic nonlinearity, and thereafter, the dynamic response is obtained by solving simultaneous nonlinear differential equations of motion using the fourth-order Runge–Kutta

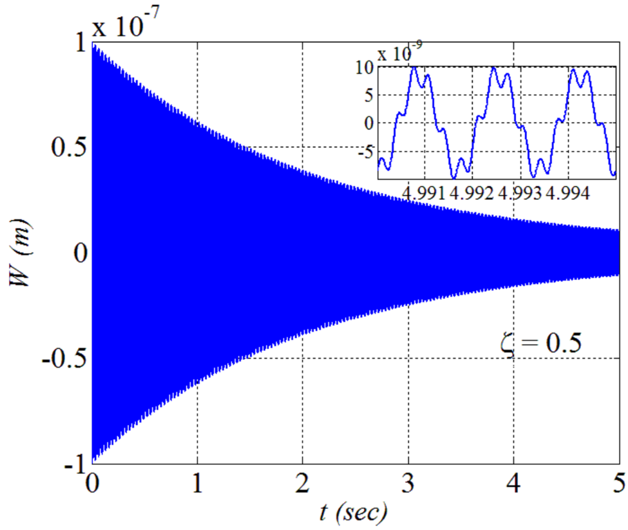

Fig. 9 Exponential decay of amplitude of nonlinear vibration of stiffened spherical panel (for $k=1$, $q=0$, ξ = 0.5, $T=100$ K, and $n_x=n_y=15$)

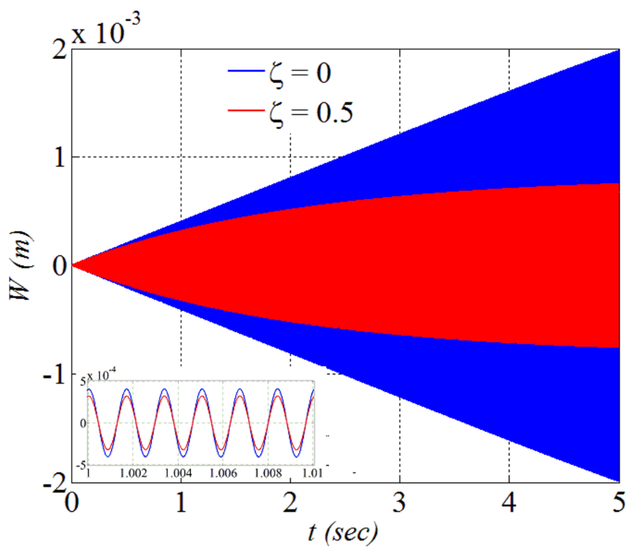

Fig. 10 Effect of damping on nonlinear vibration response of stiffened spherical panel (for $k=1$, $q=1500\sin(\Omega t)$ with / = 1, $T=100$ K, and $n_x=n_y=15$)

method. Based on the present study following important observations are revealed:

- Shell geometry is found to affect the vibration behavior prominently. Among the un-stiffened as well as stiffened FGM shell panels, the spherical shell panel exhibits the highest natural frequency with the lowest vibration amplitude, whereas lowest natural frequency with the highest amplitude is depicted by hyperbolic-paraboloidal shell.
- Irrespective of shell geometry, the natural frequencies of FGM shell panels are affected by the number of stiffeners significantly, whereas the inclusion of stiffeners reduces the amplitude of vibration considerably.
- Natural frequencies and dynamic response of un-stiffened and stiffened FGM shell panels are found to be greatly affected by material gradation profile, and at resonance conditions, higher amplitude of vibration is noticed for the increased power law index.
- An increase of temperature difference across the thickness of the shell panel reduces the natural frequency as well as increases the amplitude of vibration for all FGM shell geometries. It is attributed to the reduction of stiffness of FGM shell panels with an increase in temperature difference across the thickness of shell panel.
- Damping causes an exponential decay with time in the amplitude of unexcited vibration of stiffened FGM spherical shell panel. Further, at the resonance condition, damping causes a bound on the increase in the amplitude of stiffened FGM spherical shell panel.

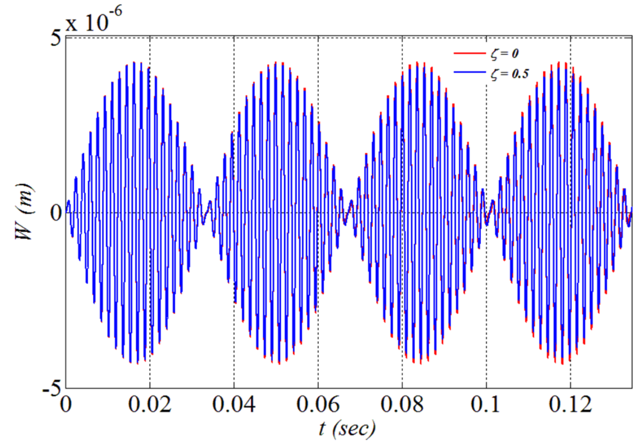

Fig. 11 Effect of damping on nonlinear vibration response (i.e., beat phenomenon) of stiffened spherical panel (for $k=1$, $q=1500$ sin (Ωt) with $\Omega/\omega=0.95$, $T=100$ K, and $n_x=n_y=15$)

Appendix

Appendix A

$$l_{11}\left(u_0\right) = \left(A_{11} + \frac{E_0 A_x}{l_x}\right) u_{0,xx} + A_{66} u_{0,yy} - K_s A_{55} C_1^2 u_0;$$

$$l_{12}(v_0) = (A_{12} + A_{66})v_{0,xy};\ l_{13}(w_0) = \left(A_{11} + \frac{E_0A_x}{l_x}\right)C_1w_{0,x} + (A_{12}C_2 + K_sA_{55}C_1)w_{0,x};$$

$$l_{14}(\phi_x) = \left(B_{11} + \frac{E_0A_xe_x}{l_x}\right)\phi_{x,xx} + B_{66}\phi_{x,yy} + K_sA_{55}C_1\phi_x,\ l_{15}(\phi_y) = (B_{12} + B_{66})\phi_{y,xy};$$

$$n_1(w_0^2) = \left(A_{11} + \frac{E_0A_x}{l_x}\right)w_{0,x}w_{0,xx} + (A_{12} + A_{66})w_{0,y}w_{0,xy} + A_{66}w_{0,x}w_{0,yy};$$

$$l_{21}(u_0) = (A_{12} + A_{66})u_{0,xy};\ l_{22}(v_0) = \left(A_{22} + \frac{E_0A_y}{l_y}\right)v_{0,yy} + A_{66}v_{0,xx} - K_sA_{44}C_2^2v_0;$$

$$l_{23}(w_0) = \left[\left(A_{22} + \frac{E_0A_y}{l_y}\right)C_2 + A_{12}C_1 + K_sA_{44}C_2\right]w_{0,y};\ l_{24}(\phi_x) = (B_{12} + B_{66})\phi_{x,xy};$$

$$l_{25}(\phi_y) = \left(B_{22} + \frac{E_0A_ye_y}{l_y}\right)\phi_{y,yy} + B_{66}\phi_{y,xx} + K_sA_{44}C_2\phi_y;$$

$$n_2(w_0^2) = \left(A_{22} + \frac{E_0A_y}{l_y}\right)w_{0,y}w_{0,yy} + A_{66}w_{0,xx}w_{0,y} + (A_{12} + A_{66})w_{0,x}w_{0,xy};$$

$$l_{31}(u_0) = -\left[\left(A_{11} + \frac{E_0A_x}{l_x}\right)C_1 + A_{12}C_2 + K_sA_{55}C_1\right]u_{0,x};\qquad l_{34}(\phi_x) = -\left[\left(B_{11} + \frac{E_0A_xe_x}{l_x}\right)C_1 + B_{12}C_2 - K_sA_{55}\right]\phi_{x,x};$$

$$l_{32}(v_0) = -\left[\left(A_{22} + \frac{E_0A_y}{l_y}\right)C_2 + A_{12}C_1 + K_sA_{44}C_2\right]v_{0,y};\qquad l_{35}(\phi_y) = -\left[\left(B_{22} + \frac{E_0A_ye_y}{l_y}\right)C_2 + B_{12}C_1 - K_sA_{44}\right]\phi_{y,y};$$

$$\begin{aligned} l_{33}(w_0) = &-\left[\left(A_{11} + \frac{E_0A_x}{l_x}\right)C_1^2 + 2A_{12}C_1C_2 - \left(A_{22} + \frac{E_0A_y}{l_y}\right)C_2^2\right]w_0 + K_sA_{55}w_{0,xx} + K_sA_{44}w_{0,yy} \\ &-N_{xx}^Tw_{0,xx} - N_{yy}^Tw_{0,yy}; \end{aligned}$$

$$\begin{aligned} n_3(w_0^2) = &\frac{1}{2}\left(A_{11} + \frac{E_0A_x}{l_x}\right)C_1w_{0,x}^2 + \frac{1}{2}\left(A_{22} + \frac{E_0A_y}{l_y}\right)C_2w_{0,y}^2 + \left(A_{11} + \frac{E_0A_x}{l_x}\right)C_1w_0w_{0,xx} + \left(A_{22} + \frac{E_0A_y}{l_y}\right)C_2w_0w_{0,yy} \\ &+\frac{1}{2}A_{12}C_1w_{0,y}^2 + \frac{1}{2}A_{12}C_2w_{0,x}^2 + A_{12}C_2w_0w_{0,xx} + A_{12}C_1w_0w_{0,yy}; \end{aligned}$$

$$n_4\left(w_0^3\right)=\frac{3}{2}\left(A_{11}+\frac{E_0A_x}{l_x}\right)w_{0,x}^2w_{0,xx}+\frac{3}{2}\left(A_{22}+\frac{E_0A_y}{l_y}\right)w_{0,y}^2w_{0,yy}+\frac{1}{2}A_{12}w_{0,x}^2w_{0,yy}+\frac{1}{2}A_{12}w_{0,y}^2w_{0,xx}$$
$$+2\left(A_{12}+2A_{66}\right)w_{0,x}w_{0,y}w_{0,xy}+A_{66}w_{0,x}^2w_{0,yy}+A_{66}w_{0,y}^2w_{0,xx};$$

$$n_5\left(u_0w_0\right)=\left(A_{11}+\frac{E_0A_x}{l_x}\right)\left(u_{0,xx}w_{0,x}+u_{0,x}w_{0,xx}\right)+\left(A_{12}+A_{66}\right)u_{0,xy}w_{0,y}+A_{12}u_{0,x}w_{0,yy}$$
$$+A_{66}u_{0,yy}w_{0,x}+2A_{66}u_{0,y}w_{0,xy};$$

$$n_6\left(v_0w_0\right)=\left(A_{22}+\frac{E_0A_y}{l_y}\right)\left(v_{0,yy}w_{0,y}+u_{0,y}w_{0,yy}\right)+\left(A_{12}+A_{66}\right)v_{0,xy}w_{0,y}+A_{12}v_{0,y}w_{0,xx}$$
$$+A_{66}v_{0,xx}w_{0,y}+2A_{66}v_{0,x}w_{0,xy};$$

$$n_7\left(w_0\phi_x\right)=\left(B_{11}+\frac{E_0A_xe_x}{l_x}\right)\left(w_{0,x}\phi_{x,xx}+w_{0,xx}\phi_{x,x}\right)+\left(B_{12}+B_{66}\right)w_{0,y}\phi_{x,xy}+B_{12}w_{0,yy}\phi_{x,x}$$
$$+B_{66}w_{0,x}\phi_{x,yy}+2B_{66}w_{0,xy}\phi_{x,y};$$

$$n_8\left(w_0\phi_y\right)=\left(B_{22}+\frac{E_0A_ye_y}{l_y}\right)\left(w_{0,y}\phi_{y,yy}+w_{0,yy}\phi_{y,y}\right)+\left(B_{12}+B_{66}\right)w_{0,x}\phi_{y,xy}+B_{12}w_{0,xx}\phi_{y,y}$$
$$+B_{66}w_{0,y}\phi_{y,xx}+2B_{66}w_{0,xy}\phi_{y,x};$$

$$l_{41}\left(u_0\right)=\left(B_{11}+\frac{E_0A_xe_x}{l_x}\right)u_{0,xx}+B_{66}u_{0,yy}+K_sA_{55}C_1u_0;$$

$$l_{42}\left(v_0\right)=\left(B_{12}+B_{66}\right)v_{0,xy};\ l_{42}\left(w_0\right)=\left[\left(B_{11}+\frac{E_0A_xe_x}{l_x}\right)C_1+B_{12}C_2-K_sA_{55}\right]w_{0,x};$$

$$l_{44}\left(\phi_x\right)=\left(D_{11}+\frac{E_0I_{xx}}{l_x}+\frac{E_0A_xe_x^2}{l_x}\right)\phi_{x,xx}+D_{66}\phi_{x,yy}-K_sA_{55}\phi_x;$$

$$l_{45}\left(\phi_y\right)=\left(D_{12}+D_{66}\right)\phi_{y,xy};$$

$$n_9\left(w_0^2\right)=\left(B_{11}+\frac{E_0A_xe_x}{l_x}\right)w_{0,x}w_{0,xx}+\left(B_{12}+B_{66}\right)w_{0,y}w_{0,xy}+B_{66}w_{0,x}w_{0,yy};$$

$$l_{51}\left(u_0\right)=\left(B_{12}+B_{66}\right)u_{0,xy};\ l_{52}\left(v_0\right)=\left(B_{22}+\frac{E_0A_ye_y}{l_y}\right)v_{0,yy}+B_{66}v_{0,xx}+K_sA_{44}C_2v_0;$$

$$l_{53}(w_0) = \left(B_{22} + \frac{E_0 A_y e_y}{l_y}\right) C_2 w_{0,y} + B_{12} C_1 w_{0,y} - K_s A_{44} w_{0,y};$$

$$l_{54}(\phi_x) = (D_{12} + D_{66})\phi_{x,xy};\ \ l_{55}(\phi_y) = \left(D_{22} + \frac{E_0 I_{yy}}{l_y} + \frac{E_0 A_y e_y^2}{l_y}\right)\phi_{y,yy} + D_{22}\phi_{y,xx} - K_s A_{44}\phi_y;$$

$$n_{10}(w_0^2) = \left(B_{22} + \frac{E_0 A_y e_y}{l_y}\right) w_{0,y} w_{0,yy} + (B_{12} + B_{66}) w_{0,x} w_{0,xy} + B_{66} w_{0,y} w_{0,xx}.$$

Appendix B

$$C_{11} = \left(A_{11} + \frac{E_0 A_x}{l_x}\right)\frac{m^2\pi^2}{a^2} + A_{66}\frac{n^2\pi^2}{b^2} + K_s A_{66} C_1^2\,,$$

$$C_{12} = (A_{12} + A_{66})\frac{mn\pi^2}{ab},\ \ C_{13} = -\left(\left(A_{11} + \frac{E_0 A_x}{l_x}\right) C_1 + A_{12} C_2 + K_s A_{66} C_1\right)\frac{m\pi}{a},$$

$$C_{14} = \left(B_{11} + \frac{E_0 A_x e_x}{l_x}\right)\frac{m^2\pi^2}{a^2} + B_{66}\frac{n^2\pi^2}{b^2} - K_s A_{66} C_1\,,\ \ C_{15} = (B_{12} + B_{66})\frac{mn\pi^2}{ab},$$

$$N_1 = -\frac{16}{9}\left[\left(A_{11} + \frac{E_0 A_x}{l_x}\right)\frac{m^2\pi}{na^3} + (A_{12} - A_{66})\frac{n\pi}{ab^2}\right],$$

$$C_{21} = (A_{12} + A_{66})\frac{mn\pi^2}{ab},\ \ C_{22} = \left(A_{11} + \frac{E_0 A_x}{l_x}\right)\frac{n^2\pi^2}{b^2} + A_{66}\frac{m^2\pi^2}{a^2} + K_s A_{66} C_2^2,$$

$$C_{23} = -\left(\left(A_{22} + \frac{E_0 A_y}{l_y}\right) C_2 + A_{12} C_1 + K_s A_{66} C_2\right)\frac{n\pi}{b},\ \ C_{24} = (B_{12} + B_{66})\frac{mn\pi^2}{ab},$$

$$C_{25} = \left(B_{22} + \frac{E_0 A_y e_y}{l_y}\right)\frac{n^2\pi^2}{b^2} + B_{66}\frac{m^2\pi^2}{a^2} - K_s A_{66} C_2\,,$$

$$C_{33} = \left(\left(A_{11} + \frac{E_0 A_x}{l_x}\right) C_1^2 + \left(A_{22} + \frac{E_0 A_y}{l_y}\right) C_2^2 + 2A_{12} C_1 C_2\right) + K_s A_{66}\left(\frac{m^2\pi^2}{a^2} + \frac{n^2\pi^2}{b^2}\right)$$

$$N_2 = -\frac{16}{9}\left[\left(A_{22} + \frac{E_0 A_y}{l_y}\right)\frac{n^2\pi}{mb^3} + (A_{12} - A_{66})\frac{m\pi}{a^2 b}\right],$$

$$C_{31} = -\left(\left(A_{11} + \frac{E_0 A_x}{l_x}\right) C_1 + A_{12} C_2 + K_s A_{66} C_1\right)\frac{m\pi}{a},$$

$$C_{32} = -\left(\left(A_{22} + \frac{E_0 A_y}{l_y}\right) C_2 + A_{12} C_1 + K_s A_{66} C_2\right)\frac{n\pi}{b},$$

$$C_{34} = -\left(\left(B_{11} + \frac{E_0 A_x e_x}{l_x}\right) C_1 + B_{12} C_2 - K_s A_{66}\right) \frac{m\pi}{a},$$

$$C_{35} = -\left(\left(B_{22} + \frac{E_0 A_y e_y}{l_y}\right) C_2 + B_{12} C_1 - K_s A_{66}\right) \frac{n\pi}{b},$$

$$C_{53} = -\left(\left(B_{22} + \frac{E_0 A_y e_y}{l_y}\right) C_2 + B_{12} C_1 - K_s A_{66}\right) \frac{n\pi}{b},$$

$$C_{54} = \left(D_{12} + D_{66}\right) \frac{mn\pi^2}{ab},$$

$$N_3 = \frac{16}{3}\left(\left(A_{11} + \frac{E_0 A_x}{l_x}\right) C_1 + A_{12} C_2\right) \frac{m}{na^2} + \frac{16}{3}\left(\left(A_{22} + \frac{E_0 A_y}{l_y}\right) C_2 + A_{12} C_1\right) \frac{n}{mb^2},$$

$$N_4 = \frac{9}{32}\left(\left(A_{11} + \frac{E_0 A_x}{l_x}\right) \frac{m^4 \pi^4}{a^4} + \left(A_{22} + \frac{E_0 A_y}{l_y}\right) \frac{n^4 \pi^4}{b^4}\right) + \left(A_{12} + 2A_{66}\right) \frac{m^2 n^2 \pi^4}{16 a^2 b^2},$$

$$N_5 = \frac{32}{9}\left(A_{66} \frac{n\pi}{ab^2} - \left(A_{11} + \frac{E_0 A_x}{l_x}\right) \frac{m^2 \pi}{na^3} - A_{12} \frac{n\pi}{ab^2}\right),$$

$$N_6 = \frac{32}{9}\left(A_{66} \frac{m\pi}{a^2 b} - \left(A_{22} + \frac{E_0 A_y}{l_y}\right) \frac{n^2 \pi}{mb^3} - A_{12} \frac{m\pi}{a^2 b}\right),$$

$$N_7 = \frac{32}{9}\left(B_{66} \frac{n\pi}{ab^2} - \left(B_{11} + \frac{E_0 A_x e_x}{l_x}\right) \frac{m^2 \pi}{na^3} - B_{12} \frac{n\pi}{ab^2}\right),$$

$$N_8 = \frac{32}{9}\left(B_{66} \frac{m\pi}{a^2 b} - \left(B_{22} + \frac{E_0 A_y e_y}{l_y}\right) \frac{n^2 \pi}{mb^3} - B_{12} \frac{m\pi}{a^2 b}\right),$$

$$C_{41} = \left(B_{11} + \frac{E_0 A_x e_x}{l_x}\right) \frac{m^2 \pi^2}{a^2} + B_{66} \frac{n^2 \pi^2}{b^2} - K_s A_{66} C_1, \quad C_{42} = \left(B_{12} + B_{66}\right) \frac{mn\pi^2}{ab},$$

$$C_{43} = -\left(\left(B_{11} + \frac{E_0 A_x e_x}{l_x}\right) C_1 + B_{12} C_2 - K_s A_{66}\right) \frac{m\pi}{a},$$

$$C_{44} = \left(D_{11} + \frac{E_0 I_{xx}}{l_x} + \frac{E_0 A_x e_x^2}{l_x}\right) \frac{m^2 \pi^2}{a^2} + D_{66} \frac{n^2 \pi^2}{b^2} + K_s A_{66},$$

$$C_{45} = \left(D_{12} + D_{66}\right) \frac{mn\pi^2}{ab}, \quad N_4 = \frac{16}{9}\left(B_{66} \frac{n\pi}{ab^2} - \left(B_{11} + \frac{E_0 A_x e_x}{l_x}\right) \frac{m^2 \pi}{na^3} - B_{12} \frac{n\pi}{ab^2}\right),$$

$$C_{51} = \left(B_{12} + B_{66}\right) \frac{mn\pi^2}{ab}, \quad C_{52} = \left(B_{22} + \frac{E_0 A_y e_y}{l_y}\right) \frac{n^2 \pi^2}{b^2} + B_{66} \frac{m^2 \pi^2}{a^2} - K_s A_{66} C_2,$$

$$C_{55} = \left(D_{22} + \frac{E_0 I_{yy}}{l_y} + \frac{E_0 A_y e_y^2}{l_y}\right) \frac{n^2 \pi^2}{b^2} + D_{66} \frac{m^2 \pi^2}{a^2} + K_s A_{66},$$

$$N_5 = \frac{16}{9}\left(B_{66} \frac{m\pi}{a^2 b} - \left(B_{22} + \frac{E_0 A_y e_y}{l_y}\right) \frac{n^2 \pi a}{mb^3} - B_{12} \frac{m\pi}{a^2 b}\right).$$

Funding Not Applicable.

Availability of data and material Not applicable.

Code availability Not applicable.

Declarations

Conflicts of interest/Competing interests On behalf of all authors, the corresponding author states that there is no conflict of interest.

References

1. Ventsel E, Krauthammer T (2001) Thin plates and shells, 1st edn. CRC Press, Boca Raton
2. Miller PR (1957) Free vibrations of a stiffened cylindrical shell. Aeronautical Research Council, London
3. Hoppmann WH (1958) Some characteristics of the flexural vibrations of orthogonally stiffened cylindrical shells. J Acoust Soc Am 30:77–82
4. Weingarten VI (1965) Free vibrations of ring-stiffened conical shells. AIAA J 3:1475–1481
5. McElman JA, Mikulas MM, Stein M (1966) Static and dynamic effects of eccentric stiffening of plates and cylindrical shells. AIAA J 4:887–894
6. Qatu MS (2002) Recent research advances in the dynamic behavior of shells: 1989–2000, Part 1: laminated composite shells. Appl Mech Rev 55:325–350
7. Nayak AN, Bandyopadhyay JN (2002) On the free vibration of stiffened shallow shells. J Sound Vib 255:357–382
8. Samanta A, Mukhopadhyay M (2004) Free vibration analysis of stiffened shells by the finite element technique. Eur J Mech A/Solids 23:159–179
9. Qu Y, Chen Y, Long X, Hua H, Meng G (2013) A modified variational approach for vibration analysis of ring-stiffened conical–cylindrical shell combinations. Eur J Mech A/Solids 37:200–215
10. Qatu MS, Sullivan RW, Wang W (2010) Recent research advances on the dynamic analysis of composite shells: 2000–2009. Compos Struct 93:14–31
11. Kumar P, Srinivasa CV (2018) On buckling and free vibration studies of sandwich plates and cylindrical shells: A review. J Thermoplast Compos Mater 33:673–724
12. Tran MT, Nguyen VL, Trinh AT (2017) Static and vibration analysis of cross-ply laminated composite doubly curved shallow shell panels with stiffeners resting on Winkler-Pasternak elastic foundations. Int J Adv Struct Eng 9:153–164
13. Chaubey AK, Kumar A, Chakrabarti A (2017) Vibration of laminated composite shells with cutouts and concentrated mass. AIAA J 56:1662–1678
14. Guo J, Shi D, Wang Q, Tang J, Shuai C (2018) Dynamic analysis of laminated doubly-curved shells with general boundary conditions by means of a domain decomposition method. Int J Mech Sci 138–139:159–186
15. Ni Z, Zhou K, Huang X, Hua H (2019) Free vibration of stiffened laminated shells of revolution with a free-form meridian and general boundary conditions. Int J Mech Sci 157–158:561–573
16. Li H, Lv H, Gu J, Xiong J, Han Q, Liu J, Qin Z (2021) Nonlinear vibration characteristics of fibre reinforced composite cylindrical shells in thermal environment. Mech Syst Signal Process 156:107665
17. Sharma K, Kumar D (2016) Nonlinear stability and failure analysis of perforated FGM plate. Indian J Pure Appl Phys 54:665–675
18. Sharma K, Kumar D (2017) Elastoplastic analysis of FGM plate with a central cutout of various shapes under thermomechanical loading. J Therm Stress 40:1417–1991
19. Sharma K, Kumar D (2018) Nonlinear stability analysis of a perforated FGM plate under thermal load. Mech Adv Mater Struct 25:100–114
20. Sasaki M, Hirai T (1991) The Centennial Memorial Issue of The Ceramic Society of Japan. Centen Meml Issue Ceram Soc Jpn 99:1002–1013
21. Miyamoto Y, Kaysser WA, Rabin BH, Kawasaki A, Ford RG (2013) Functionally graded materials: design, processing and applications. Springer Science & Business Media, Berlin
22. Wattanasakulpong N, Chaikittiratana A (2015) An analytical investigation on free vibration of FGM doubly curved shallow shells with stiffeners under thermal environment. Aerosp Sci Technol 40:181–190
23. Punera D, Kant T (2019) A critical review of stress and vibration analyses of functionally graded shell structures. Compos Struct 210:787–809
24. Kim Y-W (2015) Free vibration analysis of FGM cylindrical shell partially resting on Pasternak elastic foundation with an oblique edge. Compos Part B Eng 70:263–276
25. Khayat M, Dehghan SM, Najafgholipour MA, Baghlani A (2018) Free vibration analysis of functionally graded cylindrical shells with different shell theories using semi-analytical method. Steel Compos Struct 28:735–748
26. Li H, Pang F, Ren Y, Miao X, Ye K (2019) Free vibration characteristics of functionally graded porous spherical shell with general boundary conditions by using first-order shear deformation theory. Thin-Walled Struct. 144:106331
27. Kumar A, Kumar D (2020) Vibration analysis of functionally graded stiffened shallow shells under thermo-mechanical loading. Mater Today Proc 44:4590–4594
28. Alijani F, Amabili M, Karagiozis K, Bakhtiari-Nejad F (2011) Nonlinear vibrations of functionally graded doubly curved shallow shells. J Sound Vib 330:1432–1454
29. Shen H (2013) A Two-step perturbation method in nonlinear analysis of beams, plates and shells. Wiley, Singapore
30. Shen HS, Wang H (2014) Nonlinear vibration of shear deformable FGM cylindrical panels resting on elastic foundations in thermal environments. Compos Part B Eng 60:167–177
31. Kar VR, Panda SK (2016) Nonlinear free vibration of functionally graded doubly curved shear deformable panels using finite element method. JVC/J Vib Control 22:1935–1949
32. Kar VR, Panda SK (2017) Large-amplitude vibration of functionally graded doubly-curved panels under heat conduction. AIAA J 55:4376–4386
33. Hashemi S, Jafari A.A. (2020) An analytical solution for nonlinear vibrations analysis of functionally graded plate using modified lindstedt-poincare method. Int J Appl Mech 12(1):2050003(1-22).
34. Bich DH, Van Dung D, Nam VH (2013) Nonlinear dynamic analysis of eccentrically stiffened imperfect functionally graded doubly curved thin shallow shells. Compos Struct 96:384–395
35. Duc ND, Thang PT (2015) Nonlinear dynamic response and vibration of shear deformable imperfect eccentrically stiffened S-FGM circular cylindrical shells surrounded on elastic foundations. Aerosp Sci Technol 40:115–127
36. Dinh Duc N, Dinh Nguyen P, Dinh Khoa N (2017) Nonlinear dynamic analysis and vibration of eccentrically stiffened S-FGM elliptical cylindrical shells surrounded on elastic foundations in thermal environments. Thin-Walled Struct. 117:178–189
37. Sheng GG, Wang X (2018) The dynamic stability and nonlinear vibration analysis of stiffened functionally graded cylindrical shells. Appl Math Model 56:389–403
38. Reddy JN, Chin CD (1998) Thermomechanical analysis of functionally graded cylinders and plates. J Therm Stress 21:593–626
39. Touloukian YS (ed.) (1967), Thermophysical properties of high temperature solid materials, Macmillan, New York.
40. Javaheri R, Eslami MR (2002) Thermal buckling of functionally graded plates. AIAA J 40:162–169
41. Mindlin RD (1951) Thickness-shear and flexural vibrations of crystal plates. J Appl Phys 22:316–323
42. Vlachoutsis S (1992) Shear correction factors for plates and shells. Int J Numer Methods Eng 33:1537–1552
43. Baruch M, Singer J (1963) Effect of eccentricity of stiffeners on the general instability of stiffened cylindrical shells under hydrostatic pressure. J Mech Eng Sci 5:23–27
44. Elishakoff I, Gentilini C, Viola E (2005) Forced vibrations of functionally graded plates in the three-dimensional setting. AIAA J 43:2000–2007

45. Matsunaga H (2008) Free vibration and stability of functionally graded shallow shells according to a 2D higher-order deformation theory. Compos Struct 84:132–146
46. Alijani F, Bakhtiari-Nejad F, Amabili M (2011) Nonlinear vibrations of FGM rectangular plates in thermal environments. Nonlinear Dyn 66:251–270
47. Huang XL, Shen HS (2004) Nonlinear vibration and dynamic response of functionally graded plates in thermal environments. Int J Solids Struct 41:2403–2427
48. Huy Bich D, Dinh Duc N, Quoc Quan T (2014) Nonlinear vibration of imperfect eccentrically stiffened functionally graded double curved shallow shells resting on elastic foundation using the first order shear deformation theory. Int J Mech Sci 80:16–28
49. Duc ND, Bich DH, Cong PH (2016) Nonlinear thermal dynamic response of shear deformable FGM plates on elastic foundations. J Therm Stress 39:278–297